SPECIAL ISSUE

Biodiversity modelling reveals a significant gap between diversity hotspots and protected areas for Iranian reptiles

Sajad Noori[1] | Oliver Hawlitschek[1] | Jens Oldeland[2] | Hossein Rajaei[3] | Martin Husemann[1] | Marianna Simões[4]

[1]Leibniz Institute for the Analysis of Biodiversity Change (LIB), Hamburg, Germany

[2]Eco-Systems, Niendorfer Kirchenweg 31, Hamburg, Germany

[3]State Museum of Natural History Stuttgart, Stuttgart, Germany

[4]Senckenberg Deutsches Entomologisches Institut, Müncheberg, Germany

Correspondence
Sajad Noori, Leibniz Institute for the Analysis of Biodiversity Change (LIB), Martin-Luther-King-Platz 3, 20146 Hamburg, Germany.
Email: sajad.noori@studium.uni-hamburg.de

Abstract

The global struggle to conserve as many species as possible with limited resources requires an improvement of our knowledge on the distribution of biodiversity. In Iran, the state of knowledge is poor for most groups of organisms, except few vertebrate groups and vascular plants. Reptiles are one of the best known, most diverse vertebrate groups in Iran, with a high rate of endemism (ca. 29%), but distribution patterns and related environmental drivers remain poorly understood. In the present study, based on a large publicly available dataset, we use general additive modelling (GAM) to identify explanatory variables for species richness of reptiles in Iran. Results indicate heterogeneity parameters (range +entropy) as the variables with the highest explanatory values. Based on the grid cells of the predicted environmental richness, using hotspot analysis, we suggest seven hotspots of reptile diversity (HRDs) across the country. Our results corroborate the previously recognized HRDs and detect three additional ones, located alongside the major mountain ranges around the central deserts plateau, particularly in the Zagros Mountains. Four of the largest HRDs (ca. 90%) situate within the Irano-Anatolian and Caucasus global biodiversity hotspot. In addition, our results reveal a large gap between identified HRDs and the current network of protected areas (PAs) in the country. While three of the detected HRDs in this study are partially touched (ca. 18%) by the PA network, overall, these areas are only covered by less than 10%. Therefore, the effectiveness of the current PAs for the protection of the reptile diversity of Iran is questionable.

KEYWORDS
conservation, gap analysis, general additive modelling, herpetofauna, macroecology

-----

1 | INTRODUCTION

Biodiversity hotspots are areas featuring exceptional concentrations of endemic species while at the same time experiencing extreme loss of habitat (Brooks et al., 2006; Myers et al., 2000). Species richness and centers of endemism are critical parameters to measure the biological diversity at the macroecological scale (Arita et al., 2012; Soberon & Cavner, 2015). Thus, identifying areas with high biodiversity or conservation concerns is a crucial step toward reaching the conservation goals at global and regional scales (Burriel-Carranza et al., 2019; Sussman et al., 2019).

Two out of 36 global biodiversity hotspots extend into Iran: The Irano-Anatolian hotspot covering the western half (ca. 31%) and the Caucasus hotspots in the northern parts (ca. 3%) of the country (Anderson, 1999; CEPF, 2020; Hanson et al., 2009). However, independent pieces of evidence suggest that the current resolution of global biodiversity hotspots is too coarse to apply for conservation management purposes at the regional level (Noroozi et al., 2018; Paknia & Rajaei Sh, 2015). Therefore, defining the most diverse regions at a finer scale is an important step to conserve as many species as possible with limited resources (Cañadas et al., 2014; Mittermeier et al., 2004). Recent studies defined several biodiversity hotspots for different groups of animals and plants at a finer scale within the Irano-Anatolian and Caucasus hotspots in Iran (e.g., Noroozi et al., 2019; Yusefi et al., 2019).

The heterogeneous topography and steep climatic gradients in Iran gave rise to high rates of endemism (Gholamifard, 2011). Furthermore, its geographic position contributed to the extent mosaic of biodiversity, by sharing elements of four different zoogeographic regions: Palearctic, Euro-Siberian, Saharo-Arabian, and Oriental (Holt et al., 2013). Recent studies have reported that the biodiversity hotspots for different groups of species in the country are mostly restricted alongside two major mountain ranges in the west and north (e.g., Noroozi et al., 2019; Yusefi et al., 2019). One of them is the Zagros Mountain range, stretching from the northwest to the south and central Iran, mainly covered with xerophilous steppic oak forests. The second one is Alborz Mountain range, located along the southern shores of the Caspian Sea, hosting the Hyrcanian temperate relic. While these represent important habitats for many groups of organisms, such as mammals, birds, and most of the flora, other groups, such as reptiles, are more adapted to the vast semi-desert and desert zones in the central and south-eastern parts of the country.

Reptiles play crucial roles in many ecosystems (Burriel-Carranza et al., 2019; Pincheira-Donoso et al., 2013), and because their ranges of ecological tolerance are often narrower than those of mammals and birds, they are excellent model organisms for evolutionary, biogeographic, ecological, and conservation studies (Anderson, 1999; Pincheira-Donoso et al., 2013; Vasconcelos et al., 2012). Furthermore, they are among the best known and most diverse groups of terrestrial vertebrates in Iran with a high rate of endemism, ca. 29% (66 species; Eskandarzadeh et al., 2018). Ficetola et al. (2013) reported the Iranian plateau (including the Irano-Anatolian hotspot) as one of the most diverse regions for reptiles within the Western Palearctic. However, up to now, little attention has been paid to the geographical distribution of their diversity and to their conservation status.

In many cases, well-studied groups are the target of conservation practices, while poorly known groups will not be considered in conservation planning (Ficetola et al., 2013). The most recent checklist reported 241 species of reptiles for Iran (Safaei-Mahroo et al., 2015), which is more than most other countries in the region (e.g., Turkey, 145 species (Reptiles, 2020); Iraq, 105 species (Al-Barazengy et al., 2015); Oman,101 species (Carranza et al., 2018); and the United Arab Emirates, 60 species (Burriel-Carranza et al., 2019)). At the same time, the IUCN Red List (2020) has evaluated 64% (154 species) of the recorded reptiles for Iran; among these, 15 species were assessed as threatened species, and 35 species have not been evaluated yet (Eskandarzadeh et al., 2018; IUCN, 2020). Hence, recently, there are growing appeals for understanding the distribution patterns of reptiles in Iran (e.g., Hosseinzadeh et al., 2014; Kafash et al., 2016; Kafash et al., 2020; Kazemi & Hosseinzadeh, 2020) to provide relevant input for the delineation of conservation and management strategies.

Macroecological studies have suggested different regions of the country as hotspots of reptile diversity (HRD; e.g., Farashi & Shariati, 2017; Hosseinzadeh et al., 2014; Kafash et al., 2016, 2020). Based on 215 species of terrestrial reptile species, Hosseinzadeh et al. (2014) reported three HRDs in the southwest (the western Zagros slops), southeast, and east of the country (Figure 4). They also highlighted two centers of endemism in the west and southwest (central Zagros) of Iran. Later, Farashi and Shariati (2017) reported the Alborz and Zagros Mountains as potential hotspot regions, and Kafash et al. (2020), based on 171 species of lizards, reported three HRDs in the western Zagros Mountains, the western parts of Central Iranian Plateau, and the north-eastern parts of the country (Figure 4; Table S3). All studies showed the relevance of the Zagros Mountains (particularly its western slopes) in species isolation and diversification and HRD patterns of endemism. They also suggested that temperature is the most important predictor for the current HRDs along with other environmental factors, such as annual mean precipitation and topology (Hosseinzadeh et al., 2014; Kafash et al., 2016, 2020).

Although Hosseinzadeh et al. (2014) and Kafash et al. (2020) considered the macroecological aspect of the comprehensive reptile distribution in Iran, they did not consider how the protected areas (PA) network in the country is able to conserve the reptile fauna. However, other studies regarding conservation of some reptile species highlighted that the HRDs are not well protected by PA network in Iran (e.g., Farashi & Shariati, 2017; Kafash et al., 2016). For instance, Farashi and Shariati (2017) depicted the PA network of the country only able to protect 10% of the potential hotspots for the threatened species of the terrestrial mammals, birds, and reptiles in Iran. In addition, previous studies did not provide a clear view on which regions should be prioritized at a finer scale for conservation practices. Hosseinzadeh et al. (2014), for example, suggested a vast area alongside the boarders of Afghanistan and Pakistan as potential HRD, which includes three provinces in the eastern half. Thus, delineating consistent diverse regions is one of the first steps to propose

future priority areas for conservation and measure the effectiveness of the current PA network to concentrate conservation efforts.

We aim to close some of these gaps by using a large dataset for the distribution of reptiles in Iran, available from the public deposit Global Biodiversity Information Facility (GBIF). We modelled the distribution of reptile diversity and predict areas of specific species richness. Furthermore, environmental modelling was used to identify the most relevant environmental parameters predicting the distribution of reptile diversity, and predicted distribution of environmental richness to identify HRDs. Finally, we identified gap between detected HRDs and the current PA network in the country.

2 | MATERIALS AND METHODS

2.1 | Study area

The study area comprises the country of Iran covering roughly 1,650,000 km^2 (44°E–63°E, 25°N–40°N). We calculated species richness of reptiles at three spatial resolutions, with hexagonal grids of 4,000 km^2, 8,000 km^2, and 20,000 km^2. Hexagonal grids design (hereafter referred to as cells) was chosen, as it offers advantages over quadratic cells in terms of neighborhood distances (Birch et al., 2007). Iran covers four different UTM zones; hence, we created the cells using the EASE-Grid projection (EPSG: 6931, Brodzik et al., 2012). This ensured an equal area for all cells across the country. We created the cells with the packages *sf* (Pebesma, 2018), *rgeos* (Bivand et al., 2020), *dplyr* (Wickham et al., 2015), and *sp* (Pebesma & Bivand, 2013) in the software R v. 4.0.2 (R Core Team, 2020).

2.2 | Occurrence data

The occurrence data for reptiles of Iran, including the three orders Crocodylia, Squamata, and Testudines, were gathered from the GBIF website (GBIF, August 6, 2019). A dataset downloaded initially yielded 12,735 records (GBIF, August 6, 2019). The GBIF dataset includes the comprehensive geo-referenced dataset of 8,525 records of 146 species of lizards by Šmíd et al. (2014). After taxonomic and geographic cleaning of the records (by excluding duplications and missing values), in total, 5,687 records were retained. The dataset includes coordinate data for 245 species of reptiles, of which 235 species are Squamata (more than 98% of the occurrence records), nine Testudines (ca. 1.6% occurrence records), and one Crocodylia (< 0.2% occurrence records). All analyses were conducted at the species level. There were 24 families of reptiles in the dataset, with Gekkonidae and Lacertidae represented by every 51 species, followed by Colubridae (29 spp.), Agamidae (26 spp.), Scincidae (19 spp.), Viperidae (11 spp.), and Phyllodactylidae (10 spp.); the other families have less than six species (Table S1). Over half of the included species (53%) had more than five records in the dataset. Approximately 20% of the species (46 spp.) were endemic, and all of which belong to Squamata. Phyllodactylidae had the highest number of endemic species (80%), followed by Lacertidae (ca. 30%) and Gekkonidae (ca. 24%; Figure 1). In total, 15 species were assessed as threatened and 16 species were considered as "Data Deficient" by the IUCN Red List (IUCN, April 20, 2020), meaning that insufficient data are available to assess the risk status of these species. We created presence–absence matrices (PAM) for the species and the three hexagonal grid resolutions. Based on these PAMs, the observed species richness per cell was calculated using the R package *vegan* (Oksanen et al., 2019).
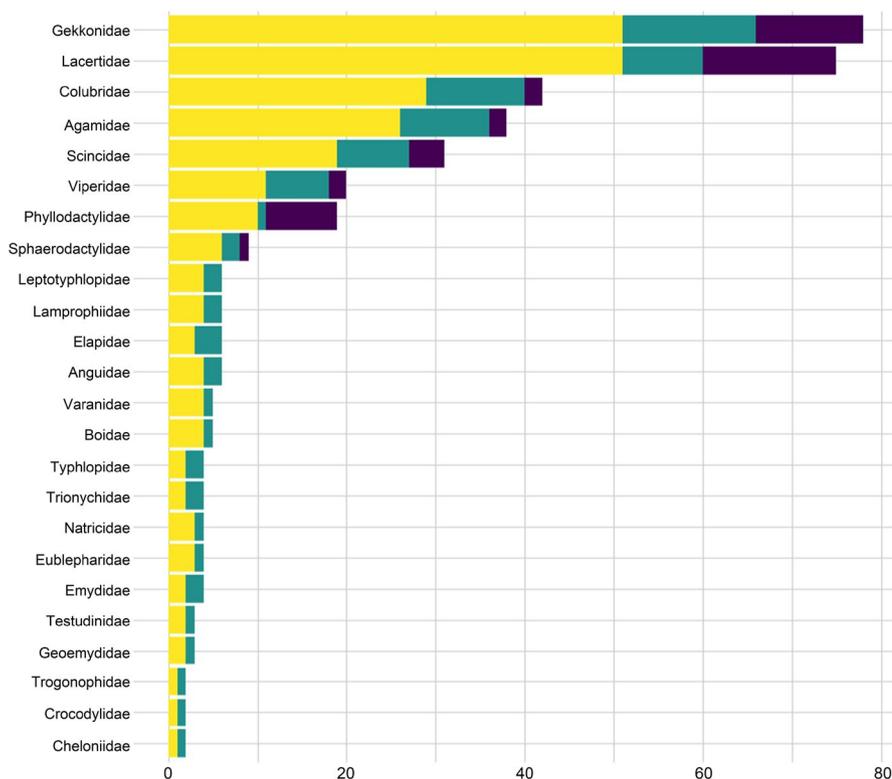

FIGURE 1 Number of endemic species (dark purple), number of genera (green), and total species number (Yellow) for each of the 24 studied families of reptiles present in Iran, included in the dataset used; yellow—total number of species, green—number of genera, and purple—number of endemic species

TABLE 1 Environmental parameters used in this study with description, unit, and source references

Theme	Parameter	Description	Unit	Source	Reference
Climate	Bio1	Annual mean temperature	°C	WorldClim 2.0	Fick & Hijmans, 2017
	Bio7	Temperature annual range	°C		
	Bio12	Annual precipitation	mm		
	Bio15	Precipitation seasonality	%		
Habitat	Entropy	Disorderliness of EVI	0–∞	EarthEnv.org	Tuanmu & Jetz, 2015
	Corr	Correlation of EVI	−1–+1		
Topography	Sha	Shannon diversity landforms	0–∞	EarthEnv.org	Amatulli et al., 2018
	VRM	Vector ruggedness measure	0–1		
	DEM	Altitude	m.a.s.l.		

Note: See references for a detailed description of how the parameters were derived. Parameters were considered as thematic sets, which then entered a model together.

2.3 | Environmental variables

For testing the richness-environment relationships, we gathered a variety of environmental variables that were found to be related to macroecological patterns of biodiversity (Table 1). These were the bioclimatic variables from the WorldClim 2.0 dataset (Fick & Hijmans, 2017), topographical variability (Amatulli et al., 2018), habitat heterogeneity (Tuanmu & Jetz, 2015) based on the remotely sensed Enhanced Vegetation Index (EVI; Huete et al., 2002), and elevation based on a global digital elevation model (Hijmans et al., 2005). All rasters were on the scale of 1 km^2, cropped, and projected to meet the extents and coordinate system of the cells. We calculated the means and standard deviations for every parameter for each cell of the hexagonal grids. We also calculated the centroid of each cell and added the metric coordinates (EPSG: 6931) as spatial predictors X and Y. For raster handling and processing, we used the additional R packages *raster* (Hijmans, 2020) and *RSAGA* (Brenning et al., 2018), which use the geoprocessing tools of the open-source software SAGA-GIS v. 7.0.1 (Conrad et al., 2015).

At each spatial scale, the environmental variable dataset for multicollinearity was checked using Pearson's correlation ®, with $r > 0.75$ as a threshold. Altitude was strongly correlated with annual mean temperature (*bio1*); however, altitude was kept, as it was not modelled within the same model as *bio1*. Standard deviation variables were correlated with the respective mean values and hence, excluded. Another strong correlation was observed between *bio1* and the Y-coordinate, but, as the coordinates will enter the models as an interaction, they were kept. On larger grid resolutions, the correlation became stronger due to the aggregation effect of increased cell size (Data S1). Multicollinearity analysis was executed with the R package *corrplot* (Wei & Simko, 2017).

2.4 | Richness–Environment models

The expected relationships between the different environmental predictors and the species richness of the cells were analyzed using generalized additive models (GAM; Wood, 2006). GAMs are very flexible in terms of the non-linear relationships that can be fitted. The model has been used in numerous recent studies to explore richness–environment relationships (e.g., Saeedi et al., 2020; Tripathi et al., 2019; Tukiainen et al., 2017). First, we created a null model, which consisted only of the mean richness value per cell. Then, we created a set of 12 GAM models that consisted of a model for every single variable, as well as three models containing all the variables belonging to a thematic set (Table 1). All environmental variables were fitted with a thin-plate spline smoother (Wood, 2006), together with spatial smoothers of the X and Y coordinates. We allowed the smoothers to be penalized to zero if the estimates did not contribute to the model; knots were kept at the default value ($k = 10$, for spatial smoother $k = 50$). All models were fitted with restricted maximum likelihood (REML) and a negative-binomial distribution, as we had overdispersal count data. Model building was done with the package *mgcv* (Wood, 2006).

The model selection was conducted using the information-theoretical framework (Burnham & Anderson, 2002) based on the Akaike information criterion (AIC; Akaike, 1973). We calculated the AIC for each of the 13 candidate models. From the AIC values, we derived delta AIC (dAIC), as well as Akaike weights (AW; scaled between 0 and 1) to identify a single best model. The best model received the lowest AIC value; subsequent models were required to have a dAIC value larger than two, and an AW substantially larger than the second model. We further calculated the deviance squared for each model, which represents the (adjusted) proportion of deviance, accounted for the model. This was required to better interpret the fit of the best model to the data. For model selection, we used the R packages *bbmle* (Bolker, 2020) and *MuMIn* (Barton, 2009).

The selected best models for residual model structure were evaluated using the standard diagnostic plots (e.g., QQ-plots, histograms, and leverage plots), the applicability of the number of knots, and their effects on the estimated degrees of freedom. To interpret, models were visualized using univariate and spatial partial regression plots. To check for potential effects of spatial autocorrelation (SAC), we analyzed the model residuals by plotting the residuals on a map and calculated isotropic, as well as anisotropic semi-variograms for the directions (0, 45, 90, and 135). Finally, we calculated a Moran's

I spatial correlogram to verify whether SAC had a strong influence at a certain distance (*lag*). *Lags* were measured in kilometers and distributed in 50 bins across the spatial extent of the study area. To conduct the model evaluation, we used the R packges *ncf* (Bjornstad & Cai, 2020), *gstat* (Pebesma, 2020), and *spdep* (Bivand et al., 2017). Model visualization was done with the *gratia* package (Simpson & Singmann, 2020) and *ggplot2* (Wickham, 2016); the summary table was built with *sjPlot* (Lüdecke, 2017). The complete analysis script is provided as Data S1.

2.5 | Biodiversity measurements and gap analysis

To measure the biodiversity of the reptile species in the country, we calculated alpha diversity of the group as the total number of species (species richness) and the number of endemic species per cell using R v. 4.0.2 (R Core Team, 2020) and QGIS v. 3.12.0 (QGIS Team, 2020). Furthermore, we used the quantitative hotspots estimation approach to delimit hotspot of reptile diversity (HRD) of Iran based on the predicted map by GAM (Sussman et al., 2019). We applied the *Getis-Ord* Statistic approach using the R package *spdep* (Bivand et al., 2017), to identify clusters on a grid weight (Getis & Ord, 1992). The resulting HRD map was used to find the overlaps between the Pas network and delineated HRDs across the country using QGIS.

All the maps in this study were generated in QGIS v. 3.12.0 (QGIS Team, 2020). The polygon vectors were obtained for Pas from Iranian Department of Environment (DOE, 2011) and Protected Planet website (Planet, 2020) and, which includes detailed information for each PA, that is, name, goal of design, area, and IUCN category. The number of species records were counted within each Pas polygon using the intersection tool in QGIS and then calculated with the R package *dplyr* (Wickham et al., 2015). The polygon files for biodiversity hotspots were downloaded from the Critical Ecosystem Partnership Fund website (CEPF, 2020).

3 | RESULTS

3.1 | Environmental models

In total, 192 models were created for the dataset using GAM modelling. As an outcome of the GAM analysis, model tests (Akaike weights and delta AIC) revealed that heterogeneity parameters (range +entropy) fit best (number of observations = 403, variation explained (R^2) = 0.279, deviance explained (D) = 35.9%), with the HRDs at 4,000 km^2 resolution (Table 2). Nevertheless, all models suggested habitat heterogeneity as the most important predictor for species richness. The ranking of the GAM models using AIC shows higher Akaike weights (AW) for range (AW = 0.8), followed by heterogeneity (AW = 0.2). In addition, our results show that the areas with higher entropy (variability) and higher enhanced vegetation index

TABLE 2 GAM models for 4,000 km^2 spatial scale

Predictors (S_{4000})	e.d.f.	ref. d.f.	z/Chi^2	p
Intercept	1.95	366.71	60.81	**<0.001**
s(X, Y)	30.31	49.00	111.70	**<0.001**
s(entropy)	4.04	9.00	35.68	**<0.001**
s(corr)	0.94	9.00	10.25	**<0.001**
n	403	–	–	–
R^2	0.279	–	–	–
D^2	35.9%	–	–	–

Note: The model estimates are presented as the effective degrees of freedom (e.d.f.), which represent the smoothness of the GAM. The reference degree of freedom (ref.d.f.) is the maximum allowed value. The z/Chi^2 are the test statistics for which the *p*-value is calculated. The bold values show that a *p*-value < 0.05 is statistically significant. For the intercept, the value is *z*-statistic while for the smoothers; the value represents the chi^2- statistic. *n* = number of observations, R^2 = variation explained, D^2 = deviance explained.
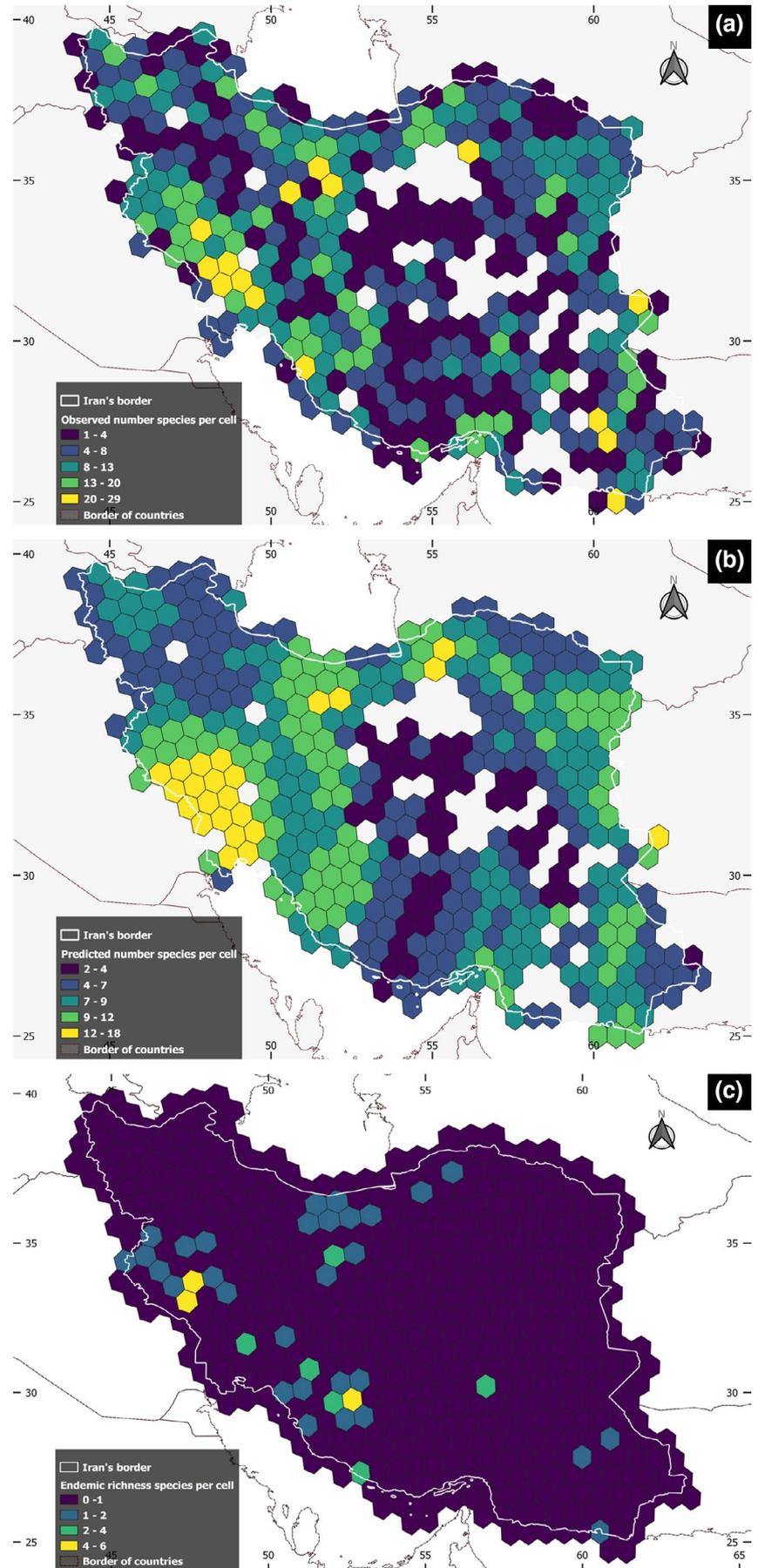
(EVI) correlation (EVI increases linearly within neighborhood cells) correlate closely with HRDs. Heterogeneity parameters were also selected as the best-fitting model for the 8,000 km^2 and 20,000 km^2 resolutions.

The validity of the models was checked using diagnostic plots and displays of the smoothers. Diagnostic plots for the residuals of the models, QQ-plot, and histogram plots depicted a normal distribution and non-linear patterns for the residuals (Data S1). There were no distinctive patterns in the plots, which showed that the data met the regression assumptions. The resulting models did not show any specific spatial autocorrelation pattern in the residuals. The diagnostic plots for 8,000 km^2 resolution show a similar pattern to the 4,000 km^2 resolution, while the residuals plots for the 20,000 km^2 showed a stronger effect of spatial autocorrelation because of low number of coordinate records, yet the validity of the model is unclear (Data S1).

3.2 | Species distribution

The smallest resolution (4,000 km^2) yielded the best predictions with an unbiased model, whereas the larger resolution results were either over smoothed, had multicollinearity or SAC issues, or explained a lower proportion of the variation (Data S1). Here, we only show the results for the 4,000 km^2 resolution. In total, there were 403 grid cells for 4,000 km^2 resolution across the study area (Figure 2). The richness of reptile species (alpha diversity) is depicted based on the observed data (Figure 2a), predicted richness using smoothed environmental proxies (Figure 2b), and observed endemic richness (endemic) per cell. The alpha-diversity maps indicated that in general the western half of the country, especially the south-western slopes of the Zagros Mountains, had the highest number of reptile species (Figure 2a). The southern parts of the

FIGURE 2 Species richness of Iranian reptiles at a resolution of 4,000 km²; (a) Observed species richness of the species per cell across the country; (b) Predicted species richness of the reptile species per cell; (c) Observed richness of endemic species per cell

Zagros Mountains also showed high species richness. The southeast of the country (Sistan-o-Baluchistan province) and southern and eastern slopes of the Alborz Mountains were also found to harbor a high diversity of reptiles.

Moreover, both observed and predicted cells for species richness show a higher alpha diversity in the southeast in comparison with central and the north of the Persian Gulf. Species richness is much higher in the northeast of Sistan-o-Baluchistan province near the Pakistan border. The southern slopes of the Alborz Mountains have a high rate of alpha diversity compared with the northern slopes; this rate decreases from west to east until the northeast of the mountain range. The observed and predicted richness maps show higher species richness in the northwest and western parts of the central desert plateau compared with other parts of the central plateau.

The richness of the endemic species (Figure 2c) is higher in the west toward the southeast of the country than in the other areas. Furthermore, the number of endemic species is high at the southern slopes of the Alborz Mountains in the north and northeast of the country. The endemic species are mainly distributed alongside two main mountain ranges (Zagros and Alborz). The

southeast regions also have a high number of endemic species alongside the Makran Mountains. The central areas around the two central deserts (Dasht-e Lut and Dasht-e Kavir deserts) have the lowest diversity of reptile species considering both richness and endemism.

3.3 | Hotspots of reptile diversity

Using the Getis-Ord Gi* statistic, we identified at least seven hotspots of reptile diversity (HRDs) based on the predicted map by GAM (Figure 3), which in total covers ca. 18% of the terrestrial areas of Iran. The biggest HRD is a vast area (ca. 125,000 km²) in the southwest covering the western slopes of the Zagros Mountains (area A; Table 3). Zagros harbors another HRD; area B is a large region (ca. 43,000 km²) in the central Zagros Mountains toward the north of the Persian Gulf. The second-largest HRD is extended from the central Alborz Mountains to the northwest of the central desert plateau (area C; ca. 64,000 km²). The eastern regions of the Alborz range encircle another HRD in the northeast (area D). The other HRDs are three smaller areas restricted to the mountain ranges in the east and
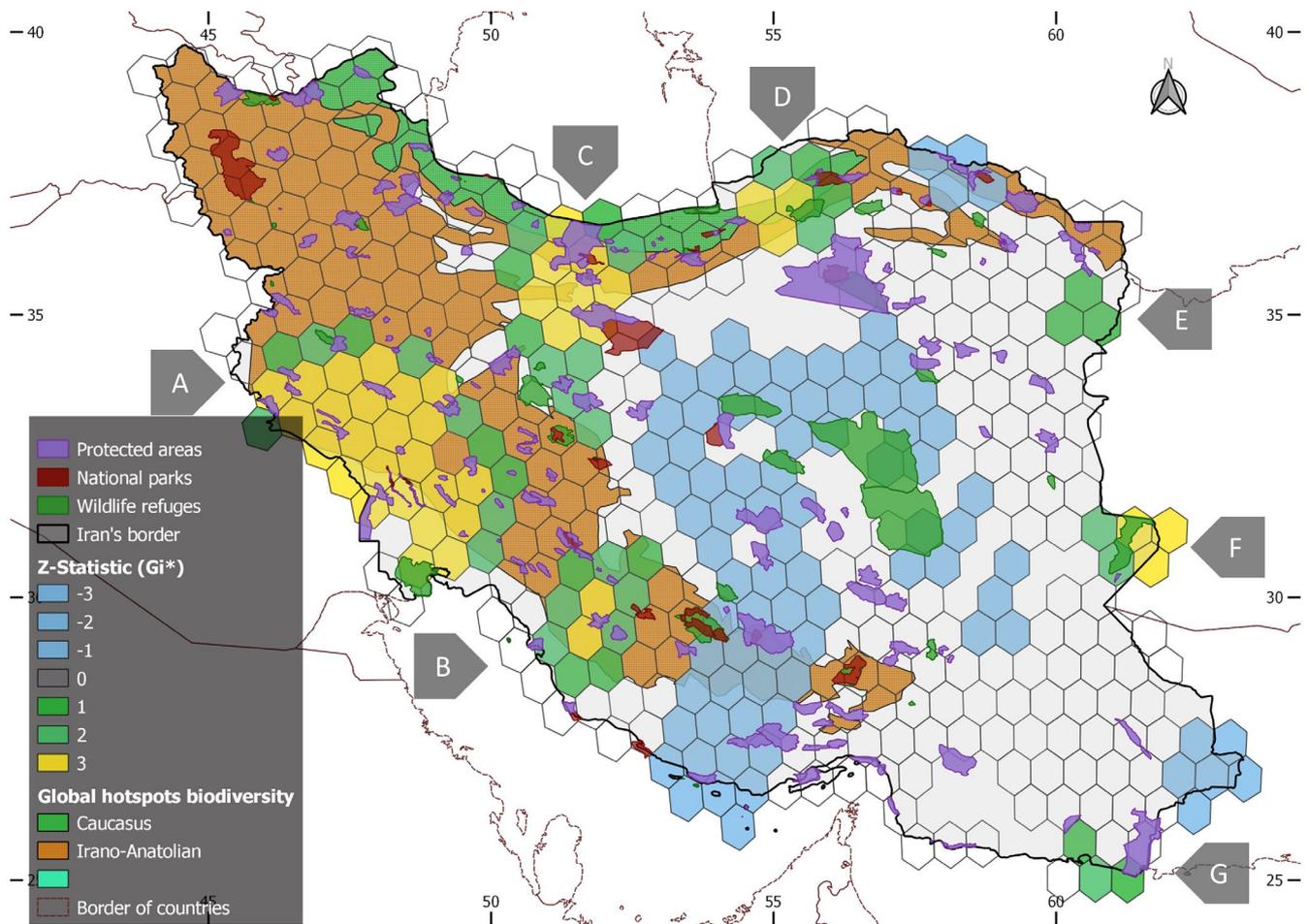

FIGURE 3 Map showing the hotspot of reptile diversity (HRD) in Iran, recovered in this study. Hexagon cell resolution of 4,000 km², clustered by weight of species richness. Values of Z-statistic (Gi*) >0 are considered as HRDs. Cells with zero scores show a random pattern, and the negative score can be regarded as a cold spot, that is, area with constantly low values

TABLE 3 Results of the gap analysis, with diversity estimates and overlaps for each global biodiversity hotspot (GBH) and the detected hotspots of reptile diversity (HRDs)

HRD	Area	#Sp.	#End.	Area Ir-An.	Area Ca.	PA
Irano-Anatolian	508407.6	135	26	0	0	46776.81
Caucasus	56389.90	46	5	0	0	6890.91
A (Khuzestan)	125379.24	87	17	101330.41	0	9981.28
B (Fars)	43759.52	54	8	32381.20	0	1971.67
C (Alborz)	64537.26	66	9	16901.84	8456.70	10326.04
D (Golestan)	26975.55	38	3	4881.22	7576.31	2597.56
E (Khorasan)	11337.13	22	1	0	0	88.78
F (Sistan)	13105.73	38	1	0	0	2975.97
G (Makran)	5289.80	24	2	0	0	907.34
Total (GBH)	564797.50	245	46	0	0	53667.72
Total (HRD)	290384.23	245	46	0	0	28848.65

Note: For each HRD, we show the area (Km^2), number of species (#sp.), number of endemic species (#End.), and area of each HRD within the Irano-Anatolian (Area Ir-An) and Caucasus (Area Ca.) GBHs, and the protected areas (PA) for each GBH and HRD with the current protected area network in Iran.
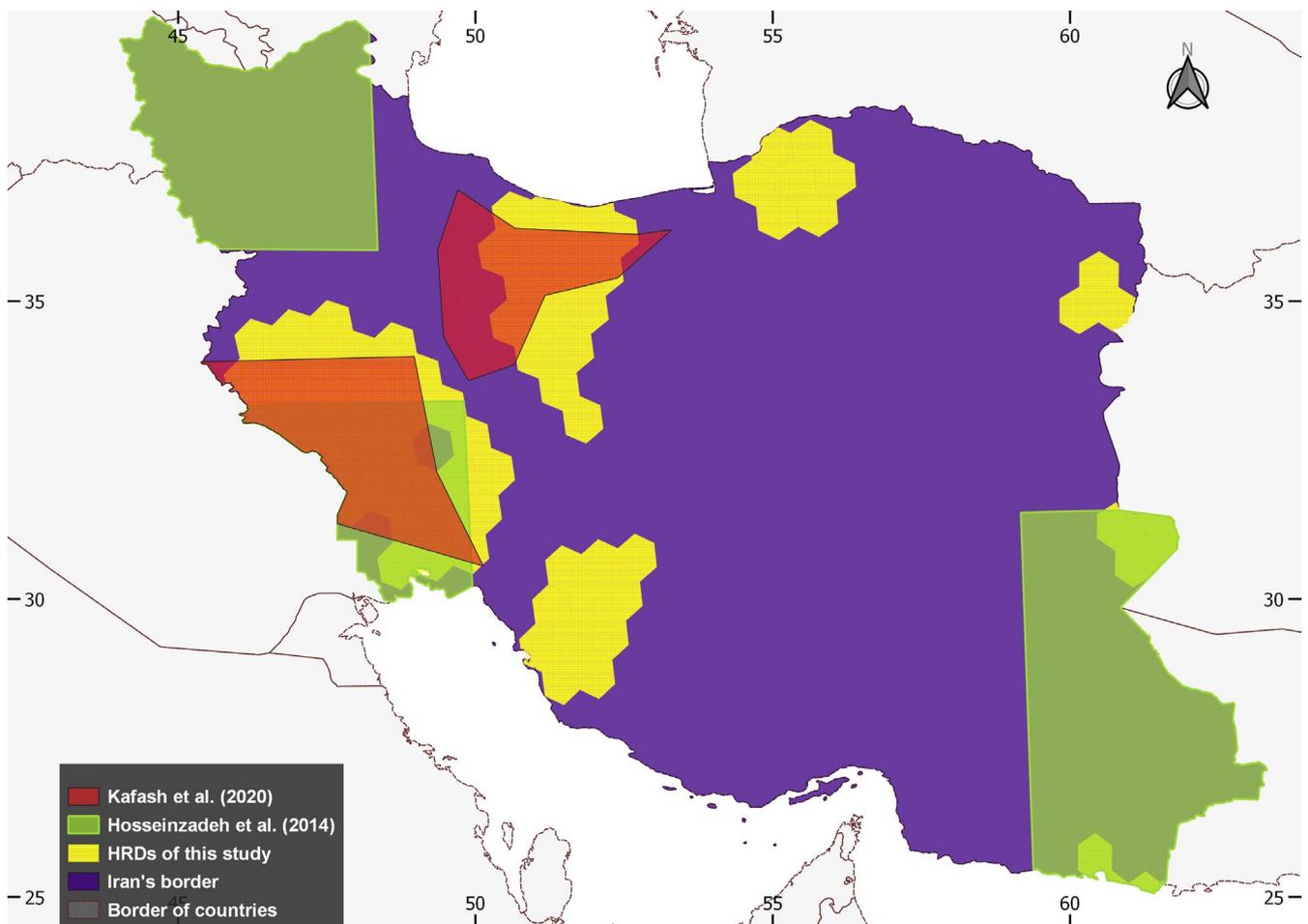

FIGURE 4 Map showing the comparison between detected hotspots of reptile diversity (HRDs) in this study (yellow), Hosseinzadeh et al. (2014) (green), and Kafash et al. (2020) (red). The area of Iran is colored purple

southeast of Iran (areas E, F, and G), at the borders with Afghanistan and Pakistan. The smallest detected HRD is area G (ca. 5,200 km^2) in the southeast of the country.

3.4 | Gap analysis

In general, detected HRDs are protected by approximately 10% and most of them are surrounded by several PAs (Table 3). None of the HRDs was fully covered by the current PA network (Figure 3). The largest HRD in the southwest of the country (area A; see Figure 3) is covered only by about 8% of the PA network, and it surrounded by several small PAs (e.g., Dez Wildlife Refuge, Karkhe Wildlife Refuge, Haft Shahidan Protected Area). On the other hand, area F has the best protection (ca. 23%); this hotspot locates in the southeast and to some extent touched by the Hamoun Protected area (Table 3). The two other HRDs with good protection are area G (ca. 17%) in the north of the Oman Sea in the southeast and area C (ca. 16%) extends from the central parts of the Alborz Mountain range toward the northwest of the central desert plateau.

Four of the detected HRDs are located within the extent of two global biodiversity hotspots (Irano-Anatolian and Caucasus; Figure 3). Areas A and B are extended within Irano-Anatolian by approximately 81% and 74%, respectively, while areas C and D area extended within both of the global biodiversity hotspots (Table 3). Irano-Anatolian and Caucasus are marginally covered by the PA network 12% and 9% respectively. However, our analyses revealed that a high number of the species were recorded in these areas (Irano-Anatolian: 135 spp. and Caucasus: 46 spp.).

Our results showed that on average, only 4.8 species have been recorded within any PA (Min = 0, Max = 69, SD = 10.5). In total, only 13% of the records were found in the PAs network. Touran (Biosphere Reserve) and Kavir (national park; two of the largest PAs in the central desert plateau) encompass more coordinate points than the other PAs in Iran, but these PAs only marginally touch HRDs (Figure 3). Three of the largest PAs in the country (Touran Biosphere Reserve, Naybandan wildlife refuge, and Lut Desert world heritage site) do cover little of the HRDs. In sum, these three PAs are 52,963 km^2 in size and represent 31% of the entire PAs network. However, none of these PAs is representative for any HRD in the country.

4 | DISCUSSION

Reptiles, despite being one of the most diverse group of taxa among the terrestrial vertebrates, have received limited attention worldwide (Böhm et al., 2013; Uri et al., 2017). Based on a large published dataset for reptiles, our study indicates habitat heterogeneity as the best predictor for species richness in Iran. We confirm the three previously proposed hotspots of reptile diversity (HRDs) and suggest four additional HRDs. Finally, our results highlighted a significant gap between the PA network and HRDs in Iran.

4.1 | Environmental explanatory drivers

Previous studies have noted the importance of different environmental factors on the distribution pattern of reptiles, for example, temperature, elevation (Hosseinzadeh et al., 2014; Kafash et al., 2020; McCain, 2010), precipitation (Luo et al., 2012; Kafash et al., 2020), topology (Burriel-Carranza et al., 2019), annual actual evapotranspiration (Ficetola et al., 2013), and normalized difference vegetation index (NDVI; Luo et al., 2012). Hence, these temperature (e.g., annual mean temperature, maximum temperature of the warmest month) and environmental variables, which have a direct correlation with ecosystem productivity (e.g., precipitation, NDVI), have a crucial influence on the species richness of reptiles (Burriel-Carranza et al., 2019; Kafash et al., 2020).

Our results, however, show that climatic variables (i.e., temperature and precipitation) and topology are valuable predictors for the distribution of Iranian reptile species (e.g., Hosseinzadeh et al., 2014; Kafash et al., 2020), but heterogeneity parameters (i.e., range +entropy) are the best explanatory variables regarding species-rich regions, explaining 28% of variation for the current dataset. The heterogeneity parameter represents a standardized measure of habitat diversity to study the heterogeneity–biodiversity relationships at conservation planning scales (Stein et al., 2014). Heterogeneity parameters have been introduced as a powerful tool to better understand patterns of biodiversity distribution, highly relevant with respect to biophysical characteristics and biodiversity (García-Llamaset et al., 2018; Kerr & Packer, 1997).

4.2 | Regions of high reptile diversity

Our results corroborate the suggested HRDs in the country (Hosseinzadeh et al., 2014; Kafash et al., 2020; Kazemi & Hosseinzadeh, 2020), but add further regions, mainly located alongside the two main mountain ranges in Iran (Alborz and Zagros). This agrees with the findings of other studies, which found the western slopes of the Zagros Mountain range to be the largest HRD in Iran (Hosseinzadeh et al., 2014; Kafash et al., 2020; Sindaco & Jeremcenko, 2008). Four of the largest HRDs (Figure 3; Areas A, B, C, and D) are restricted to the Irano-Anatolian and Caucasus global biodiversity hotspots in the western half and the north of the country, which can be defined as hotspots within a hotspot (Cañadas et al., 2014). The Irano-Anatolian region formerly has been determined as one of the important HRDs of the western Palearctic (Ficetola et al., 2013). In addition to the previously detected HRDs in the Zagros Mountains, HRD B (Figure 3) in the central part of the Zagros Mountains range (Fars Province) has not been detected in previous studies. However, Hosseinzadeh et al. (2014) had already defined this area as a region with high endemism. Most of the regions with high endemism in this study overlap with HRD areas (Figure 2c). Our results (Figure 2b) suggest more potential regions of high endemism in the Central Alborz, northeast, and southeast of the country (Figure 2c).

Our study further detected two new HRDs in the southeast of Iran, more specifically in the northeast (area F) and south (area G) of the Sistan-o-Baluchistan Province. The richness of endemic species also indicates high diversity for reptiles in this province, particularly along with the Makran Mountains (Figure 3b). This mountain range extends between Iran and Pakistan and acts as a barrier restricting moisture entering from the Oman Sea and the Indian Ocean to the central desert plateau of Iran (Noroozi et al., 2018). Hosseinzadeh et al. (2014) have defined these HRDs (corresponding to our areas E, F, and G) as one big hotspot in the eastern half of Iran along the borders of Afghanistan and Pakistan (Figure 4; Table 1). A strong influence of the oriental biogeographic realm has been proposed for these regions (Anderson, 1999). Our study has been unable to detect the HRD in the northwest of the country (Azerbaijan), which Hosseinzadeh et al. (2014) reported earlier. This HRD was likewise not detected in Kafash et al. (2020). A possible explanation for this may be the use of different datasets. Kafash et al. (2020) used the same GBIF dataset as we used in this study (Šmíd et al., 2014).

Several studies documented that worldwide mountain areas generally harbor the most diverse regions (Cañadas et al., 2014; Graham et al., 2005; Noroozi et al., 2016). Altogether, our results suggest that all the defined HRDs of Iranian reptiles are restricted to mountainous areas. Mountainous areas in Iran provide high habitat diversity and heterogeneity allowing for high species diversity (Anderson, 1999). The Zagros Mountain range has been suggested as the most diverse region for different animal and plant species in Iran (e.g., Kafash et al., 2020; Kazemi & Hosseinzadeh, 2020; Noroozi et al., 2016, 2019; Yusefi et al., 2019). With the uplifting of the Zagros about 22 million years ago, a wide range of unoccupied microhabitats opened up and caused isolation to other parts of the country hence providing the prerequisite for the evolution of new species (Mouthereau, 2011). The Zagros can be not only considered a melting pot of different bioregions as it represents the barrier, but also the contact zone of the Mesopotamian fauna and the central Iranian plateau (Gholamifard, 2011; Kafash et al., 2016, 2020; Kazemi & Hosseinzadeh, 2020). In addition, Quaternary climatic oscillations had a remarkable influence on the current biodiversity composition in Iran (Kafash et al., 2020; Rajaei et al., 2013).

4.3 | Conservation gap

Pas are the main tool for habitat and species conservation and their location is crucial to protect as much biodiversity as possible with the available resources. However, often there is a gap between biodiversity-rich regions and protected areas due to human–wildlife conflicts and different criteria to define the priority areas (Sussman et al., 2019). Estimating the gap between the delineated HRDs and the established Pas network will help to assess the efficiency of Pas in the country (Vasconcelos et al., 2012). As depicted in Figure 3, some of the largest Pas are restricted to the remote and uninhabited regions in the central deserts, that is, the Lut Desert World Heritage Site (natural or mixed; ca. 22,650 km²), Naybandan (Wildlife Refuge;

ca. 15,372 km²), and Touran, the largest PA of Iran (Protected Area; ca. 14,932 km²). However, most of the HRDs (ca. 90% of the area) are distributed in the western half and north, which harbor most of the populated areas.

It seems possible that the PA network in Iran, similar to most other countries, has been designed in the view of charismatic species, that is, mammals and birds (Rodrigues et al., 2004; Coad et al., 2019). However, studies have suggested the current PA network does not even protect mammals in the region sufficiently well (e.g., Farashi & Shariati, 2017; Farashi et al., 2017; Yusefi et al., 2019). A comparison between the Pas in Iran and two global biodiversity hotspots (Irano-Anatolian and Caucasus) shows that the PA network only covers ca. 10% of these areas (DOE, 2011; Planet, 2020). These areas encompass ~60% of the total detected HRD areas in this study (areas A, B, C, and D; Table 3). The mentioned HRDs (areas A, B, C, and D) are the largest HRD in Iran (ca. 90%), including a high number of reptile species and a high rate of endemism (Eskandarzadeh et al., 2018; Kazemi & Hosseinzadeh, 2020). In average, these HRDs are only covered by ca. 10% of the current PA network of the country (Table 3). Therefore, none of the defined HRDs is well protected by current Pas (Figure 3). While areas G, C, and F are partially touched by the PA network, two of the largest HRDs, areas A and B, which are 58% out of total HRDs' area, are on average covered by several small protected areas (6%).

The assessment of the gap analysis even in the developed countries indicated that reptiles are one of the less protected vertebrate groups (Maiorano et al., 2006; Uri et al., 2017). For instance, terrestrial reptiles are even poorly represented in the PA network (ca. 15%) in the nationally designated protected areas and the pan-European Natura 2000 network across Europe (Abellán & Sánchez-Fernández, 2015). Even though the number of Pas in Iran has increased in number and size (10.12% of the country's surface) since 1950, recent studies reported that approximately one-quarter (22%) of the Pas in the country are under heavy anthropogenic pressure, particularly in the western half and northern part of Iran (Karimi & Jones, 2020; Kolahi et al., 2012). These areas are compatible with the Irano-Anatolian hotspot and four of the biggest HRDs (areas A, B, C, and D). Besides the poor protection of the PA network, livestock overgrazing, illegal logging, poaching, mining, etc. are among the most important threats regarding the effectiveness of Pas (Hodjat et al., 2019; Kolahi et al., 2012; Soofi et al., 2018). Therefore, the current Pas network does not protect the HRDs sufficiently well in Iran.

5 | CONCLUSIONS

Our work confirms previous studies that, at a finer scale, there are several hotspots of reptile diversity (HRDs) within the global biodiversity hotspots (Irano-Anatolian and Caucasus) in Iran. Furthermore, our results provide additional unrecognized HRDs for the country. High environmental heterogeneity and intensive contrast of climate and topology resulted in rich biodiversity in these areas. Our results

show that heterogeneity factors (range +entropy) are the best explanatory variables for the distribution of the species richness in the study area. Although defined HRDs are mainly restricted to the mountain ranges in the Irano-Anatolian and Caucasus global biodiversity hotspots, our results depicted that the current network of protected areas does not protect these highly diverse regions sufficiently well. In addition, these areas currently are under high anthropogenic pressure. Therefore, an assessment of the conservation status of Iranian reptiles and urgent management actions are required.

CONFLICT OF INTEREST

The authors declare that they have no conflict of interest.

AUTHOR CONTRIBUTIONS

SN, OH, JO, MH, and MS involved in conceptualization. JO, SN, and MS involved in methodology. SN, JO, and MS involved in investigation. SN, OH, JO, HR, MH, and MS involved in writing original draft preparation. OH, JO, HR, MH, MS involved in writing supervision. All authors read and approved the final manuscript.

ORCID

Sajad Noori https://orcid.org/0000-0002-9933-6713

Oliver Hawlitschek https://orcid.org/0000-0001-8010-4157

Jens Oldeland https://orcid.org/0000-0002-7833-4903

Hossein Rajaei https://orcid.org/0000-0002-3940-3734

Martin Husemann https://orcid.org/0000-0001-5536-6681

Marianna Simões https://orcid.org/0000-0003-4401-5530

REFERENCES

Abellán, P., & Sánchez-Fernández, D. (2015). A gap analysis comparing the effectiveness of Natura 2000 and national protected area networks in representing European amphibians and reptiles. *Biodiversity and Conservation*, 24(6), 1377–1390. https://doi.org/10.1007/s10531-015-0862-3

Akaike, H. (1973). Maximum likelihood identification of gaussian autoregressive moving average models. *Biometrika*, 60(2), 255–265. https://doi.org/10.1093/biomet/60.2.255

Al-Barazengy, A. N., Salmon, A. O., & Hameed, F. T. A. (2015). Updated list of Amphibians and Reptiles in Iraq 2014. *Bulletin of the Iraq Natural History Museum*, 13(4), 29–40. https://jnhm.uobaghdad.edu.iq/index.php/BINHM/article/view/65

Amatulli, G., Domisch, S., Tuanmu, M. N., Parmentier, B., Ranipeta, A., Malczyk, J., & Jetz, W. (2018). Data Descriptor: A suite of global, cross-scale topographic variables for environmental and biodiversity modeling. *Scientific Data*, 5, 1–15. https://doi.org/10.1038/sdata.2018.40

Anderson, S. C. (1999). *The lizards of Iran* (Vol. 6, pp. 1–442). Society for the Study of Amphibians and Reptiles.

Arita, H. T., Christen, A., Rodríguez, P., & Soberón, J. (2012). The presence-absence matrix reloaded: The use and interpretation of range-diversity plots. *Global Ecology and Biogeography*, 21(2), 282–292. https://doi.org/10.1111/j.1466-8238.2011.00662.x

Barton, K. (2009). *MuMIn: multi-model inference. R package version 1. 0. 0.* Retrieved from https://cran.r-project.org/web/packages/MuMIn/index.html

Birch, C. P. D., Oom, S. P., & Beecham, J. A. (2007). Rectangular and hexagonal grids used for observation, experiment and simulation in ecology. *Ecological Modelling*, 206(3–4), 347–359. https://doi.org/10.1016/j.ecolmodel.2007.03.041

Bivand, R., Altman, M., Anselin, L., Assunção, R., Berke, O., Bernat, A., & Blanchet, G. (2017). *'spdep'. R package version 0.6-13*. Retrieved from https://r-forge.r-project.org/projects/spdep/

Bivand, R., Rundel, C., Pebesma, E., Stuetz, R., Hufthammer, K. O., & Bivand, M. R. (2020). *rgeos: Interface to Geometry Engine-Open 564 Source ('GEOS'). R package version 0.5-5.* Retrieved from https://cran.r-project.org/web/packages/rgeos/index.html

Bjornstad, O. N., & Cai, J. (2020). *ncf: Spatial Covariance Functions. R package Version 1.2-9.* Retrieved from https://cran.r-project.org/web/packages/ncf/index.html

Bolker, M. B. (2020). *"bbmle": Title Tools for General Maximum Likelihood Estimation Description Methods and functions for fitting maximum likelihood models in R. R package version 1.0.23.1.* Retrieved from https://Github.Com/Bbolker/Bbmle

Böhm, M., Collen, B., Baillie, J. E., Bowles, P., Chanson, J., Cox, N., Hammerson, G., Hoffmann, M., Livingstone, S. R., Ram, M., Rhodin, A. G. J., Stuart, S. N., Dijk, P. P., Young, B. E., Afuang, L. E., Aghasyan, A., Aguilar, A. G. C., Ajtic, R., Akarsu, F., … Zug, G. (2013). The conservation status of the world's reptiles. *Biological conservation*, 157, 372–385.

Brenning, A., Bangs, D., Becker, M., Schratz, P., & Polakowski, F. (2018). *RSAGA: SAGA geoprocessing and terrain analysis. R package version 1.2. 0.* Retrieved from https://cran.r-project.org/web/packages/RSAGA/index.html

Brodzik, M. J., Billingsley, B., Haran, T., Raup, B., & Savoie, M. H. (2012). EASE-Grid 2.0: Incremental but significant improvements for earth-gridded data sets. *ISPRS International Journal of Geo-Information*, 1(1), 32–45. https://doi.org/10.3390/ijgi1010032

Brooks, T. M., Mittermeier, R. A., Da Fonseca, G. A. B., Gerlach, J., Hoffmann, M., Lamoreux, J. F., Mittermeier, C. G., Pilgrim, J. D., & Rodrigues, A. S. L. (2006). Global biodiversity conservation priorities. *Science*, 313(5783), 58–61. https://doi.org/10.1126/science.1127609

Burnham, K. P., & Anderson, D. R. (2002). *Model selection and multimodel inference* (2nd ed., p. 488). Springer.

Burriel-Carranza, B., Tarroso, P., Els, J., Gardner, A., Soorae, P., Mohammed, A. A., Tubati, S. R. K., Eltayeb, M. M., Shah, J. N., Tejero-Cicuéndez, H., Simó-Riudalbas, M., Pleguezuelos, J. M., Fernández-Guiberteau, D., Šmíd, J., & Carranza, S. (2019). An integrative assessment of the diversity, phylogeny, distribution, and conservation of the terrestrial reptiles (Sauropsida, Squamata) of the United Arab Emirates. *PLoS ONE*, 14(5), 1–36. https://doi.org/10.1371/journal.pone.0216273

Cañadas, E. M., Fenu, G., Peñas, J., Lorite, J., Mattana, E., & Bacchetta, G. (2014). Hotspots within hotspots: Endemic plant richness, environmental drivers, and implications for conservation. *Biological Conservation*, 170, 282–291. https://doi.org/10.1016/j.biocon.2013.12.007

Carranza, S., Xipell, M., Tarroso, P., Gardner, A., Arnold, E. N., Robinson, M. D., Simó-Riudalbas, M., Vasconcelos, R., de Pous, P., Amat, F., Šmíd, J., Sindaco, R., Metallinou, M., Els, J., Pleguezuelos, J. M., Machado, L., Donaire, D., Martínez, G., Garcia-Porta, J., ... Al Akhzami, S. N. (2018). Diversity, distribution and conservation of the terrestrial reptiles of Oman (Sauropsida, Squamata). *PLoS ONE*, *13*(2), 1–31. https://doi.org/10.1371/journal.pone.0190389

CEPF (2020). *The Critical Ecosystem Partnership Fund*. Retrieved from https://www.cepf.net/

Coad, L., Watson, J. E., Geldmann, J., Burgess, N. D., Leverington, F., Hockings, M., Knights, K., & Di Marco, M. (2019). Widespread shortfalls in protected area resourcing undermine efforts to conserve biodiversity. *Frontiers in Ecology and the Environment*, *17*(5), 259–264.

Conrad, O., Bechtel, B., Bock, M., Dietrich, H., Fischer, E., Gerlitz, L., Wehberg, J., Wichmann, V., & Böhner, J. (2015). System for automated geoscientific analyses (SAGA) v. 2.1.4. *Geoscientific Model Development Discussions*, *8*(2), 2271–2312. https://doi.org/10.5194/gmdd-8-2271-2015

DOE (2011). *Department of Environment, Islamic Republic of Iran*. Retrieved from https://en.doe.ir

Eskandarzadeh, N., Rastegar-Pouyani, N., Rastegar-Pouyani, E., Fathinia, B., Bahmani, Z., Hamidi, K., & Gholamifard, A. (2018). Annotated checklist of the endemic Tetrapoda species of Iran. *Zoosystema*, *40*(sp1), 507–537. https://doi.org/10.5252/zoosystema2018v40a24

Farashi, A., & Shariati, M. (2017). Biodiversity hotspots and conservation gaps in Iran. *Journal for Nature Conservation*, *39*, 37–57. https://doi.org/10.1016/j.jnc.2017.06.003

Farashi, A., Shariati, M., & Hosseini, M. (2017). Identifying biodiversity hotspots for threatened mammal species in Iran. *Mammalian Biology*, *87*, 71–88. https://doi.org/10.1016/j.mambio.2017.06.002

Ficetola, G. F., Bonardi, A., Sindaco, R., & Padoa-Schioppa, E. (2013). Estimating patterns of reptile biodiversity in remote regions. *Journal of Biogeography*, *40*(6), 1202–1211. https://doi.org/10.1111/jbi.12060

Fick, S. E., & Hijmans, R. J. (2017). WorldClim 2: new 1-km spatial resolution climate surfaces for global land areas. *International Journal of Climatology*, *37*(12), 4302–4315. https://doi.org/10.1002/joc.5086

García-Llamaset, P., Calvo, L., la Cruz, M., & Suárez-Seoane, S. (2018). Landscape heterogeneity as a surrogate of biodiversity in mountain systems: What is the most appropriate spatial analytical unit? *Ecological Indicators*, *85*, 285–294. https://doi.org/10.1016/j.ecolind.2017.10.026

GBIF (2019). *GBIF.org (06 August 2019) GBIF Occurrence Download*. https://doi.org/10.15468/dl.jyxmyq

Getis, A., & Ord, J. (1992). The analysis of spatial association by use of distance statistics. *Grographical Analysis*, *24*(3), 189–206. https://doi.org/10.1111/j.1538-4632.1992.tb00261.x

Gholamifard, A. (2011). Endemism in the reptile fauna of Iran. *Iranian Journal of Animal Biosystematics*, *7*(1), 13–29.

Graham, C. H., Smith, T. B., & Languy, M. (2005). Current and historical factors influencing patterns of species richness and turnover of birds in the Gulf of Guinea highlands. *Journal of Biogeography*, *32*(8), 1371–1384. https://doi.org/10.1111/j.1365-2699.2005.01284.x

Hanson, T., Brooks, T. M., Da Fonseca, G. A. B., Hoffmann, M., Lamoreux, J. F., MacHlis, G., Mittermeier, C. G., Mittermeier, R. A., & Pilgrim, J. D. (2009). Warfare in biodiversity hotspots. *Conservation Biology*, *23*(3), 578–587. https://doi.org/10.1111/j.1523-1739.2009.01166.x

Hijmans, R. J. (2020). *raster: Geographic Data Analysis and Modeling. R package vresion 3.4-5*. Retrieved from https://cran.r-project.org/web/packages/raster/index.html

Hijmans, R. J., Cameron, S. E., Parra, J. L., Jones, P. G., & Jarvis, A. (2005). Very high resolution interpolated climate surfaces for global land areas. *International Journal of Climatology*, *25*(15), 1965–1978. https://doi.org/10.1002/joc.1276

Hodjat, S. H., Saboori, A., & Husemann, M. (2019). A view on the historic and contemporary acridid fauna (Orthoptera: Caelifera: Acrididae) of Iran-A call for conservation efforts. *Journal of Crop Protection*, *8*(2), 135–142. https://jcp.modares.ac.ir/article-3-25563-en.html

Holt, B. G., Lessard, J. P., Borregaard, M. K., Fritz, S. A., Araujo, M. B., Dimitrov, D., & Nogués-Bravo, D. (2013). An update of Wallace's zoogeographic regions of the world. *Science*, *339*(6115), 74–78. https://www.science.org/doi/full/10.1126/science.1228282

Hosseinzadeh, M. S., Aliabadian, M., Rastegar-Pouyani, E., & Rastegar-Pouyani, N. (2014). The roles of environmental factors on reptile richness in Iran. *Amphibia-Reptilia*, *35*(2), 215–225. https://doi.org/10.1163/15685381-00002946

Huete, A., Didan, K., Miura, T., Rodriguez, E. P., Gao, X., & Ferreira, L. G. (2002). Overview of the radiometric and biophysical performance of the MODIS vegetation indices. *Remote Sensing of Environment*, *83*(1–2), 195–213. https://doi.org/10.1016/S0034-4257(02)00096-2

IUCN (2020). *IUCN Red List*. Retrieved from https://www.iucnredlist.org/

Kafash, A., Ashrafi, S., Yousefi, M., Rastegar-Pouyani, E., Rajabizadeh, M., Ahmadzadeh, F., Grünig, M., & Pellissier, L. (2020). Reptile species richness associated to ecological and historical variables in Iran. *Scientific Reports*, *10*(1), 1–11. https://doi.org/10.1038/s41598-020-74867-3

Kafash, A., Kaboli, M., Koehler, G., Yousefi, M., & Asadi, A. (2016). Ensemble distribution modeling of the mesopotamian spiny-tailed lizard, saara loricata (Blanford, 1874), in iran: An insight into the impact of climate change. *Turkish Journal of Zoology*, *40*(2), 262–271. https://journals.tubitak.gov.tr/zoology/abstract.htm?id=18096

Karimi, A., & Jones, K. (2020). Assessing national human footprint and implications for biodiversity conservation in Iran. *Ambio*, *49*(9), 1506–1518. https://doi.org/10.1007/s13280-019-01305-8

Kazemi, S. M., & Hosseinzadeh, M. S. (2020). High diversity and endemism of herpetofauna in the Zagros mountains. *ECOPERSIA*, *8*(4), 221–229. https://ecopersia.modares.ac.ir/article-24-38921-en.html

Kerr, J. T., & Packer, L. (1997). Habitat heterogeneity as a determinant of mammal species richness in high-energy regions. *Nature*, *385*, 252–254. https://doi.org/10.1038/385252a0

Kolahi, M., Sakai, T., Moriya, K., & Makhdoum, M. F. (2012). Challenges to the future development of Iran's protected areas system. *Environmental Management*, *50*(4), 750–765. https://doi.org/10.1007/s00267-012-9895-5

Luo, Z., Tang, S., Li, C., Fang, H., Hu, H., Yang, J., Ding, J., & Jiang, Z. (2012). Environmental effects on vertebrate species richness: Testing the energy, environmental stability and habitat heterogeneity hypotheses. *PLoS ONE*, *7*(4), e35514.

Lüdecke, D. (2017). *'sjPlot': Data Visualization for Statistics in Social Science. R package version 2.4.0 October*. Retrieved from https://Github.Com/Strengejacke/SjPlot

Maiorano, L., Falcucci, A., & Boitani, L. (2006). Gap analysis of terrestrial vertebrates in Italy: Priorities for conservation planning in a human dominated landscape. *Biological Conservation*, *133*(4), 455–473. https://doi.org/10.1016/j.biocon.2006.07.015

McCain, C. M. (2010). Global analysis of reptile elevational diversity. *Global Ecology and Biogeography*, *19*(4), 541–553. https://doi.org/10.1111/j.1466-8238.2010.00528.x

Mittermeier, R. A., Gil, P. R., Hoffman, M., Pilgrim, J., Brooks, T., Mittermeier, C., Lamoreux, J., Da Fonseca, G. A. B., & Saligmann, P. A. (2004). *Hotspots Revisited: Earth's Biologically Richest and Most Endangered Terrestrial Ecoregions Cemex*. Mexico City.

Mouthereau, F. (2011). Timing of uplift in the Zagros belt/Iranian plateau and accommodation of late Cenozoic Arabia-Eurasia convergence. *Geological Magazine*, *148*(5–6), 726–738. https://doi.org/10.1017/S0016756811000306

Myers, N., Mittermeier, R. A., Mittermeier, C. G., Da Fonseca, G. A., & Kent, J. (2000). Biodiversity hotspots for conservation priorities. *Nature*, *403*(6772), 853–858. https://doi.org/10.1038/35002501

Noroozi, J., Moser, D., & Essl, F. (2016). Diversity, distribution, ecology and description rates of alpine endemic plant species from Iranian mountains. *Alpine Botany*, *126*(1), 1–9. https://doi.org/10.1007/s00035-015-0160-4

Noroozi, J., Talebi, A., Doostmohammadi, M., Manafzadeh, S., Asgarpour, Z., & Schneeweiss, G. M. (2019). Endemic diversity and distribution of the Iranian vascular flora across phytogeographical regions, biodiversity hotspots and areas of endemism. *Scientific Reports*, *9*(1), 1–12. https://doi.org/10.1038/s41598-019-49417-1

Noroozi, J., Talebi, A., Doostmohammadi, M., Rumpf, S. B., Linder, H. P., & Schneeweiss, G. M. (2018). Hotspots within a global biodiversity hotspot-areas of endemism are associated with high mountain ranges. *Scientific Reports*, *8*(1), 1–10. https://doi.org/10.1038/s41598-018-28504-9

Oksanen, J., Blanchet, F. G., Friendly, M., Kindt, R., Legendre, P., McGlinn, D., Minchin, P. R., O'Hara, R. B., Simpson, G. L., & Solymos, P. (2019). *vegan: Community Ecology Package. R package version 2.5. 4. 2019*. Retrieved from https://Cran.r-Project.Org/Web/Packages/Vegan/Index.Html

Paknia, O., & Rajaei Sh, H. (2015). Geographical patterns of species richness and beta diversity of Larentiinae moths (Lepidoptera: Geometridae) in two temperate biodiversity hotspots. *Journal of Insect Conservation*, *19*(4), 729–739. https://doi.org/10.1007/s10841-015-9795-0

Pebesma, E. (2018). *sf: Simple Features for R. R package version 0.6-3*. Retrieved from https://cran.r-project.org/web/packages/sf/index.html

Pebesma, E. J. (2020). *'gstat': Spatial and Spatio-Temporal Geostatistical Modelling, Prediction and Simulation. R Package version 2.0-6*. Retrieved from https://Github.Com/r-Spatial/Gstat/

Pebesma, E., & Bivand, R. (2013). *'sp': classes and methods for spatial data Author. R package version 1.0-13 Date*. Retrieved from https://cran.r-project.org/web/packages/sp/index.html

Pincheira-Donoso, D., Bauer, A. M., Meiri, S., & Uetz, P. (2013). Global taxonomic diversity of living reptiles. *PLoS One*, *8*(3), 1–10. https://doi.org/10.1371/journal.pone.0059741

Planet, P. (2020). *Protected Area Profile for Iran (Islamic Republic Of) from the World Database of Protected Areas*. Retrieved from https://www.protectedplanet.net/country/IR

QGIS Team (2020). *QGIS Geographic Information System. Open Source Geospatial Foundation Project. (3.14)*. Retrieved from http://qgis.osgeo.org

R Core Team (2020). *R: A language and environment for statistical computing. R Foundation for Statistical Computing (4.0.2)*. Retrieved from https://www.r-project.org/

Rajaei Sh, H., Rödder, D., Weigand, A. M., Dambach, J., Raupach, M. J., & Wägele, J. W. (2013). Quaternary refugia in southwestern Iran: Insights from two sympatric moth species (Insecta, Lepidoptera). *Organisms Diversity and Evolution*, *13*(3), 409–423. https://doi.org/10.1007/s13127-013-0126-6

Reptiles (2020). *The Reptile database*. Retrieved from http://www.reptile-database.org/

Rodrigues, A. S. L., Akçakaya, H. R., Andelman, S. J., Bakarr, M. I., Boitani, L., Brooks, T. M., Chanson, J. S., Fishpool, L. D. C., Da Fonseca, G. A. B., Gaston, K. J., Hoffmann, M., Marquet, P. A., Pilgrim, J. D., Pressey, R. L., Schipper, J., Sechrest, W., Stuart, S. N., Underhill, L. G., Waller, R. W., ... Yan, X. (2004). Global gap analysis: Priority regions for expanding the global protected-area network. *BioScience*, *54*(12), 1092–1100. https://doi.org/10.1641/0006-3568(2004)054[1092:GGAPRF]2.0.CO;2

Saeedi, H., Simões, M., & Brandt, A. (2020). Biodiversity and distribution patterns of deep-sea fauna along the temperate NW Pacific. *Progress in Oceanography*, *183*, 102296. https://doi.org/10.1016/j.pocean.2020.102296

Safaei-Mahroo, B., Ghaffari, H., Fahimi, H., Yazdanian, S. B. M., Majd, E. N., Rezazadeh, S. S. H. Y. E., Hosseinzadeh, M. S., Nasrabadi, R., Rajabizadeh, M., Mashayekhi, M., Motesharei, A., Nader, A., & Kazemi, S. M. (2015). The herpetofauna of Iran: Checklist of taxonomy, distribution and conservation status. *Asian Herpetological Research*, *6*(4), 257–290. https://doi.org/10.16373/j.cnki.ahr.140062

Simpson, G. L., & Singmann, H. (2020). *gratia: Graceful 'ggplot'-Based Graphics and Other Functions for GAMs Fitted Using "mgcv". R package 0.4.1*. Retrieved from https://cran.r-project.org/web/packages/gratia/index.html

Sindaco, R., & Jeremcenko, V. K. (2008). *The reptiles of the western Palearctic: annotated checklist and distri- butional atlas of the turtles, crocodiles, amphisbaenians and lizards of Europe, North Africa, Middle East and Central Asia* (Vol. 1).

Šmíd, J., Moravec, J., Kodym, P., Kratochvíl, L., Yousefkhani, S. S. H., & Frynta, D. (2014). Annotated checklist and distribution of the lizards of Iran. *Zootaxa*, *3855*(1), 1–97. https://www.biotaxa.org/Zootaxa/article/view/zootaxa.3855.1.1

Soberon, J., & Cavner, J. (2015). Indices of biodiversity pattern based on presence-absence matrices: A GIS implementation. *Biodiversity Informatics*, *10*, 22–34. https://doi.org/10.17161/bi.v10i0.4801

Soofi, M., Ghoddousi, A., Zeppenfeld, T., Shokri, S., Soufi, M., Jafari, A., Ahmadpour, M., Qashqaei, A. T., Egli, L., Ghadirian, T., Chahartaghi, N. R., Zehzad, B., Kiabi, B. H., Khorozyan, I., Balkenhol, N., & Waltert, M. (2018). Livestock grazing in protected areas and its effects on large mammals in the Hyrcanian forest, Iran. *Biological Conservation*, *217*, 377–382. https://doi.org/10.1016/j.biocon.2017.11.020

Stein, A., Gerstner, K., & Kreft, H. (2014). Environmental heterogeneity as a universal driver of species richness across taxa, biomes and spatial scales. *Ecology Letters*, *17*(7), 866–880. https://doi.org/10.1111/ele.12277

Sussman, A. L., Gardner, B., Adams, E. M., Salas, L., Kenow, K. P., Luukkonen, D. R., Monfils, M. J., Mueller, W. P., Williams, K. A., Leduc-Lapierre, M., & Zipkin, E. F. (2019). A comparative analysis of common methods to identify waterbird hotspots. *Methods in Ecology and Evolution*, *10*(9), 1454–1468. https://doi.org/10.1111/2041-210X.13209

Tripathi, P., Behera, M. D., & Roy, P. S. (2019). Spatial heterogeneity of climate explains plant richness distribution at the regional scale in India. *PLoS ONE*, *14*(6), 1–16. https://doi.org/10.1371/journal.pone.0218322

Tuanmu, M. N., & Jetz, W. (2015). A global, remote sensing-based characterization of terrestrial habitat heterogeneity for biodiversity and ecosystem modelling. *Global Ecology and Biogeography*, *24*(11), 1329–1339. https://doi.org/10.1111/geb.12365

Tukiainen, H., Alahuhta, J., Field, R., Ala-Hulkko, T., Lampinen, R., & Hjort, J. (2017). Spatial relationship between biodiversity and geodiversity across a gradient of land-use intensity in high-latitude landscapes. *Landscape Ecology*, *32*(5), 1049–1063. https://doi.org/10.1007/s10980-017-0508-9

Uri, R., Feldman, A., Novosolov, M., Allison, A., & Bauer, A. M. (2017). The global distribution of tetrapods reveals a need for targeted reptile conservation. *Nature Ecology & Evolution*, *1*(11), 1677–1682. https://doi.org/10.1038/s41559-017-0332-2

Vasconcelos, R., Brito, J. C., Carvalho, S. B., Carranza, S., & James Harris, D. (2012). Identifying priority areas for island endemics using genetic versus specific diversity - The case of terrestrial reptiles of the Cape Verde Islands. *Biological Conservation*, *153*, 276–286. https://doi.org/10.1016/j.biocon.2012.04.020

Wei, T., & Simko, V. (2017). *R package "corrplot": Visualization of a Correlation Matrix (Version 0.84)*. Retrieved from https://Github.Com/Taiyun/Corrplot

Wickham, H. (2016). *ggplot2: elegant graphics for data analysis*. Springer.

Wickham, H., Francois, R., Henry, L., & Müller, K. (2015). *dplyr: A Grammar of Data Manipulation. R package version 0.4. 3.* Retrieved from https://cran.r-project.org/web/packages/dplyr/index.html

Wood, S. N. (2006). Generalized additive models: an introduction with R. Chapman and Hall/CRC. *Texts in Statistical Science, 67,* 391.

Yusefi, G. H., Faizolahi, K., Darvish, J., Safi, K., & Brito, J. C. (2019). The species diversity, distribution, and conservation status of the terrestrial mammals of Iran. *Journal of Mammalogy, 100*(1), 55–71. https://doi.org/10.1093/jmammal/gyz002

SUPPORTING INFORMATION

Additional supporting information may be found online in the Supporting Information section.

Table S1. Complete list of the studied species in our dataset.

Table S2. A comparison between the results of our (General Additive Modelling (GAM)) at three spatial scales (4000, 8000, and 2000 km^2).

Table S3. A comparison between detected HRD locations in this study and defined potential hotspot areas in previous studies.

Data S1. Complete steps in R programming environment for the GAM analyses at scale of 4000 km^2 and the results of the analyses.

Figure S1. The multicollinearity analysis using Pearson's correlation coefficient to find the correlated predictors. a) the complete multicollinearity analysis. b) The analysis exclude correlation coefficient less than 0.75.

Figure S2. The distribution map of the occurrence records based on the observed data (a) and predicted data (b) at 4000 km^2 scale.

Figure S3. The graph shows the correlation between observed and our prediction for distribution for the reptile species in Iran.

Figure S4. The evaluation for residual model structure of the best model using diagnostic plots. a) QQ-plots. b & d) leverage plots. c) Histogram plot.

Figure S5. Univariate and spatial partial regression plots to interpret better the models.

Figure S6. Analysis of the model residuals by plotting the residuals on a map to check for potential effects of spatial autocorrelation (SAC).

Figure S7. Analysis of the model residuals by calculating isotropic, as well as anisotropic semi-variograms to check for potential effects of spatial autocorrelation (SAC).

Figure S8. Analysis of the model residuals by calculating isotropic, as well as anisotropic semi-variograms for the directions (0, 45, 90, and 135) to check for potential effects of spatial autocorrelation (SAC).

Figure S9. Calculation a Moran's I spatial correlogram to verify whether SAC had a strong influence at a certain distance (lag). Lags were measured in kilometres and distributed in 50 bins across the spatial extent of the study area.

Biodiversity modelling reveals a significant gap between diversity hotspots and protected areas for Iranian reptiles

Sajad Noori, Oliver Hawlitschek, Jens Oldeland, Hossein Rajaei, Martin Husemann & Marianna Simões

Supporting Information

- **Table S1**. Complete list of the studied species in our dataset
- **Table S2**. A comparison between the results of our (General Additive Modelling (GAM)) at three spatial scales (4000, 8000, and 2000 km^2)
- **Table S3**. A comparison between detected HRD locations in this study and defined potential hotspot areas in previous studies
- **Data S1**. The complete steps in R programming environment for the GAM analyses at scale of 4000 km2 and the results of the analyses

Table S1. Complete list of the studied species in our dataset

Table S1. The list of the species names and number of the records for each species from GBIF (GBIF, 06 August 2019).

Order	Family	Species	Subspecies	Number of records
Crocodylia	Crocodylidae	*Crocodylus palustris*	*palustris*	9
Squamata	Agamidae	*Agama sp.*		5
		Calotes versicolor		6
		Laudakia sp.		3
		Laudakia melanura	*lirata*	3
		Laudakia melanura		2
		Laudakia nupta	*nupta*	123
		Laudakia nupta		114
		Laudakia nupta	*fusca*	7
		Paralaudakia caucasia		223
		Paralaudakia erythrogaster		15
		Paralaudakia microlepis		44
		Paralaudakia stoliczkana		1
		Phrynocephalus		2
		Phrynocephalus ananjevae		2
		Phrynocephalus arabicus		2
		Phrynocephalus helioscopus	*helioscopus*	7
		Phrynocephalus helioscopus		4
		Phrynocephalus maculatus		52
		Phrynocephalus mystaceus		18
		Phrynocephalus ornatus		15
		Phrynocephalus ornatus	*vindumi*	2
		Phrynocephalus persicus		48
		Phrynocephalus scutellatus		228
		Pseudotrapelus sinaitus		1
		Saara asmussi		22
		Saara loricata		44
		Stellio sp.		5
		Trapelus agilis		317
		Trapelus agilis	*agilis*	70
		Trapelus agilis	*khuzistanensis*	26
		Trapelus ruderatus		148
		Trapelus sanguinolentus		6
		Uromastyx aegyptia		6
		Anguis cephallonica	*fragilis*	1
		Anguis colchica		35
		Anguis colchica	*colchicus*	2
		Anguis fragilis		3
		Pseudopus apodus		55
	Boidae	*Eryx sp.*		2
		Eryx jaculus	*jaculus*	1

	Eryx jayakari		4
	Eryx tataricus		2
	Eryx tataricus	*tataricus*	1
Colubridae	*Boiga trigonata*		1
	Coluber sp.		9
	Coluber andreanus		1
	Eirenis sp.		4
	Eirenis collaris		1
	Eirenis collaris	*collaris*	1
	Eirenis coronella		1
	Eirenis coronella	*coronella*	1
	Eirenis persicus		7
	Eirenis punctatolineatus		1
	Eirenis rechingeri		1
	Elaphe dione		1
	Elaphe quatuorlineata		1
	Hemorrhois ravergieri		1
	Lytorhynchus diadema		1
	Lytorhynchus maynardi		2
	Lytorhynchus ridgewayi		4
	Platyceps karelini		4
	Platyceps najadum		4
	Platyceps rhodorachis		9
	Platyceps ventromaculatus		1
	Rhynchocalamus ilamensis		3
	Rhynchocalamus melanocephalus		2
	Rhynchocalamus satunini	*satunini*	1
	Spalerosophis sp.		2
	Spalerosophis diadema		11
	Spalerosophis diadema	*cliffordii*	3
	Spalerosophis microlepis		1
	Telescopus fallax		4
	Telescopus nigriceps		1
	Telescopus tessellatus		2
	Telescopus tessellatus	*tessellatus*	2
	Zamenis persicus		3
Elapidae	*Hydrophis viperinus*		1
	Pelamis platura		1
	Walterinnesia aegyptia		2
Eublepharidae	*Eublepharis angramainyu*		40
	Eublepharis macularius		1
	Eublepharis turcmenicus		2
Gekkonidae	*Agamura sp.*		1
	Agamura persica		80
	Bunopus sp.		3

Bunopus crassicauda			54
Bunopus tuberculatus			150
Crossobamon eversmanni			11
Crossobamon eversmanni	*eversmanni*		1
Crossobamon eversmanni	*lumsdenii*		1
Cyrtodactylus sp.			1
Cyrtopodion sp.			8
Cyrtopodion agamuroides			22
Cyrtopodion brevipes			5
Cyrtopodion gastrophole			27
Cyrtopodion golubevi			2
Cyrtopodion hormozganum			1
Cyrtopodion kachhense			3
Cyrtopodion kiabii			3
Cyrtopodion kirmanense			10
Cyrtopodion persepolense			2
Cyrtopodion scabrum			126
Cyrtopodion sistanense			5
Hemidactylus flaviviridis			35
Hemidactylus persicus			62
Hemidactylus robustus			24
Hemidactylus romeshkanicus			1
Mediodactylus sp.			1
Mediodactylus aspratilis			20
Mediodactylus heterocercus			19
Mediodactylus heteropholis			6
Mediodactylus ilamensis			1
Mediodactylus russowii			7
Mediodactylus sagittifer			7
Mediodactylus spinicauda			8
Mediodactylus stevenandersoni			5
Microgecko chabaharensis			2
Microgecko helenae			22
Microgecko helenae	*helenae*		20
Microgecko helenae	*fasciatus*		6
Microgecko latifi			21
Microgecko persicus			12
Microgecko persicus	*persicus*		10
Microgecko persicus	*bakhtiari*		4
Parsigecko ziaiei			2
Rhinogecko femoralis			1
Pseudoceramodactylus khobarensis			3
Rhinogecko misonnei			11
Stenodactylus affinis			16
Stenodactylus arabicus			2

	Stenodactylus doriae		25
	Tenuidactylus caspius		71
	Tenuidactylus longipes		23
	Tenuidactylus turcmenicus		1
	Tenuidactylus voraginosus		1
	Trigonodactylus sp.		1
	Tropiocolotes sp.		20
	Tropiocolotes hormozganensis		2
	Tropiocolotes naybandensis		2
Lacertidae	*Acanthodactylus sp.*		3
	Acanthodactylus blanfordii		78
	Acanthodactylus boskianus		10
	Acanthodactylus cantoris		10
	Acanthodactylus grandis		11
	Acanthodactylus khamirensis		1
	Acanthodactylus micropholis		34
	Acanthodactylus nilsoni		3
	Acanthodactylus schmidti		14
	Apathya cappadocica	*urmiana*	20
	Apathya cappadocica		3
	Apathya yassujica		4
	Darevskia caspica		11
	Darevskia chlorogaster		23
	Darevskia defilippii		44
	Darevskia kamii		5
	Darevskia kopetdaghica		3
	Darevskia praticola		5
	Darevskia raddei		17
	Darevskia raddei	*raddei*	12
	Darevskia raddei	*chaldoranensis*	10
	Darevskia schaekeli		5
	Darevskia steineri		6
	Eremias sp.		76
	Eremias acutirostris		6
	Eremias andersoni		3
	Eremias arguta		9
	Eremias fasciata		53
	Eremias grammica		15
	Eremias intermedia		11
	Eremias kavirensis		2
	Eremias lalezharica		7
	Eremias lineolata		27
	Eremias montana		5
	Eremias nigrocellata		43
	Eremias papenfussi		2

	Eremias persica		194
	Eremias pleskei		19
	Eremias strauchi		72
	Eremias suphani		1
	Iranolacerta sp.		1
	Iranolacerta brandtii		32
	Iranolacerta zagrosica		5
	Lacerta sp.		2
	Lacerta media		40
	Lacerta media	*media*	1
	Lacerta mostoufii		2
	Lacerta strigata		53
	Mesalina sp.		1
	Mesalina brevirostris		17
	Mesalina brevirostris	*fieldi*	4
	Mesalina guttulata		6
	Mesalina watsonana		422
	Ophisops sp.		3
	Ophisops elegans		414
	Ophisops elegans	*elegans*	4
	Timon princeps		24
Lamprophiidae	*Malpolon monspessulanus*		1
	Psammophis sp.		2
	Psammophis lineolatus		1
	Psammophis schokari		9
	Leptotyphlops		2
	Leptotyphlops nursii		1
	Myriopholis blanfordi		1
	Myriopholis macrorhyncha		3
Natricidae	*Natrix sp.*		1
	Natrix natrix		5
	Natrix natrix	*persa*	2
	Natrix tessellata		14
	Natrix tessellata	*tessellata*	2
Phyllodactylidae	*Asaccus sp.*		3
	Asaccus andersoni		1
	Asaccus elisae		51
	Asaccus granularis		1
	Asaccus griseonotus		13
	Asaccus kermanshahensis		2
	Asaccus kurdistanensis		2
	Asaccus nasrullahi		5
	Asaccus tangestanensis		3
	Asaccus zagrosicus		1
Scincidae	*Ablepharus bivittatus*		25
	Ablepharus bivittatus	*bivittatus*	1

		Ablepharus pannonicus	91
		Chalcides ocellatus	6
		Eumeces blythianus	1
		Eumeces schneideri	*princeps*	56
		Eumeces schneideri		21
		Eumeces schneideri	*zarudnyi*	12
		Eurylepis taeniolata	8
		Mabuya sp.	1
		Ophiomorus	2
		Ophiomorus blanfordi	2
		Ophiomorus brevipes	20
		Ophiomorus maranjabensis	3
		Ophiomorus nuchalis	4
		Ophiomorus persicus	7
		Ophiomorus streeti	5
		Ophiomorus tridactylus	10
		Scincus scincus	*conirostris*	7
		Scincus scincus		6
		Trachylepis aurata	*transcaucasica*	49
		Trachylepis aurata		8
		Trachylepis septemtaeniata		101
		Trachylepis septemtaeniata	*septemtaeniata*	1
		Trachylepis vittata	6
Sphaerodactylidae	*Pristurus rupestris*		40
		Pristurus rupestris	*iranicus*	1
Sphaerodactylidae	*Teratoscincus sp.*		6
Sphaerodactylidae	*Teratoscincus bedriagai*		26
Sphaerodactylidae	*Teratoscincus keyserlingii*		61
Sphaerodactylidae	*Teratoscincus microlepis*		9
Sphaerodactylidae	*Teratoscincus scincus*		10
Trogonophidae	*Diplometopon zarudnyi*		8
Typhlopidae	*Typhlops sp.*		2
		Xerotyphlops vermicularis	9
Varanidae	*Varanus sp.*		1
		Varanus bengalensis	12
		Varanus bengalensis	*bengalensis*	1
		Varanus griseus		49
		Varanus griseus	*caspius*	9
		Varanus griseus	*griseus*	3
		Varanus nesterovi	1
Viperidae	*Agkistrodon sp.*		1
		Echis carinatus	22
		Echis coloratus	1
		Gloydius halys	4
		Gloydius halys	*caucasicus*	1
		Gloydius intermedius	4

		Macrovipera lebetina	*obtusa*	2
		Montivipera latifii		1
		Pseudocerastes persicus		2
		Pseudocerastes urarachnoides		2
		Vipera sp.		2
		Vipera berus		1
Testudines	Cheloniidae	*Chelonia mydas*		1
	Emydidae	*Emys orbicularis*		16
		Trachemys scripta	*elegans*	3
	Geoemydidae	*Mauremys sp.*		2
		Mauremys caspica		18
		Mauremys caspica	*caspica*	10
	Testudinidae	*Testudo graeca*		33
		Testudo graeca	*ibera*	3
		Testudo horsfieldii		7
	Trionychidae	*Amyda cartilaginea*		1
		Rafetus euphraticus		1

- **Table S2**. A comparison between the results of our (General Additive Modelling (GAM)) at three spatial scales (4000, 8000, and 2000 km²)

Table S2. GAM models at scale 4,000, 8,000, and 20,000 km² spatial scale. The model estimates are presented as the effective degrees of freedom (e.d.f.), which represent the smoothness of the GAM. The reference degree of freedom (ref.d.f.) is the maximum allowed value. The z/Chi² are the test statistics for which the p-value is calculated. For the intercept, the value is z-statistic while for the smoothers; the value represents the Chi²-statistic. n = number of observations, R² = variation explained, D²= deviance explained

Predictors	4000 km²		8000 km²		20,000 km²	
	Log-Mean	P	Log-Mean	P	Log-Mean	P
Intercept	1.95	<0.001	2.360	<0.001	2.870	<0.001
Smooth term (X,Y)	30.310	<0.001	7.520	<0.001	0.000	0.742
Smooth term (entropy)	4.040	<0.001	2.420	<0.001	4.420	<0.001
Smooth term (corr)	0.940	<0.001	2.700	<0.001	-	-
Observations	403		228		105	
R²	0.279		0.195		0.172	
Deviance	36.232		228.717		108.934	

- **Table S3**. A comparison between detected HRD locations in this study and defined potential hotspot areas in previous studies

Table S3. Location of the Detected hotspots of reptile diversity (HRDs) in the current study, Hosseinzadeh et al. (2014), and Kafash et al. (2020). In our study, we detected seven HRDs, from which three of them had been suggested by the other studies.

High diverse areas	Current study	Hosseinzadeh et al. 2014	Kafash et al. 2020
Zagros Mountains: Western slopes of Zagros mountain in the west and southwest of Iran	HRD A	Southwest of Iran in Khuzestan Plain	Western Zagros Mountains
Zagros Mountains: Central Zagros and the north of the Persian Gulf	HRD B	-	-
Alborz Mountains: Central Alborz, North west and North of Central Plateau	HRD C	-	North eastern and north western of Central Iranian Plateau
Alborz Mountains: North east of Iran, eastern of the Alborz Mountains	HRD D	-	-
Khorasan-e-Jonobi Province: East of Iran on the border with Afghanistan	HRD E	-	-
Sistan and Baluchistan Province: North east of the Sistan-va - Baluchistan Province on the borders with Afghanistan and Pakistan	HRD F	East of Iran	-
Makran Mountains: Sothern regions, North of the Oman Sea, along with Makran Mountains	HRD G	East of Iran	
Azerbaijan: Northwest of Iran	-	North and Northwest of Iran	-

Data S1. The complete steps in R programming environment for the GAM analyses at scale of 4000 km^2 and the results of the analyses

   In this work, we applied the GAM at three spatial scales on our dataset at 4000, 8000, and 2000 km^2. Here we provide the complete R script steps and resulted graphs only for scale of 4000 km^2, which can be easily applied for all the scales by changing the gridded scale shape file (which here it is marked with * in the R script).

   Step 1. First, we need to load all required packages.

```
### General
library(sf) # load shp and add centroids
library(corrplot) # multicollinearity

### GAM modelling and model selection
library(mgcv) # gam model
library(bbmle) # AICtab
library(MuMIn) # Weight for Akaike Weight

### Model evaluation
library(broom) # glance
library(modEvA) # Dsquared
library(gratia) # plotting GAMs
library(sjPlot) # final summary table

#### Spatial Autocorrelation (SAC)
library(gstat) # variograms + bubble plot
library(sp) # spatial data handling

library(spdep) # Morans I
library(ncf) # SAC correlogram
```

   Step 2. In this step, we start the analysis by preparing the data set. This includes loading the data from a shapefile into R, adding the coordinates of a cells centroid (in meters), and removing an outlier which is present in the MODIS EVI-correlation measure. The latter is then log-scaled to remove a strong skew in the data. Different shapefiles for each scales can be imported in the working directory line (*).

```
## read shapefile with sf
*hex_env <- read_sf("F:the Working directory/hex_pam_4000.shp")
## add X Y coordinates in meters with EPSG 6931
mycentroids <- st_transform(hex_env, 6931) %>%
st_centroid() %>%
# this is the crs from d, which has no EPSG code:
st_transform(., '+proj=longlat +ellps=WGS84 +no_defs') %>%
# since you want the centroids in a second geometry col:
st_geometry()
df2 = data.frame(st_coordinates(mycentroids))
## add coordinates to sf
hex_env$X<-df2$X
hex_env$Y<-df2$Y

### remove an outlier in correlation measure
hex_env <- subset(hex_env, corr > 1000)
```

```
### put correlation measure on log-scale
hex_env$corr <- log(hex_env$corr)

## make data.frame for modelling
envonly <- st_drop_geometry(hex_env)
envonly <- envonly[,-1]
```

Step 3. Next, we will analyse the multicollinearity of the data using Pearson's correlation coefficient (Figure S1a). As this plot is hard to read, we will restrict the figure to values beyond r = abs (0.75; Figure S1b).

```
M <- cor(envonly[,-c(17:18)],use = "pairwise.complete.obs")

corrplot(cor(envonly[,-c(17:18)],
      use = "pairwise.complete.obs"),method = "color",
      addCoef.col="white",order = "AOE",
      number.cex=0.75,tl.cex = 1 )
```

By looking at these two figures, we see that the standard deviation (*sd*) values often correlate more or less strong with the mean values (Figure S1b). Hence, we ignore the sd values from now on. Bio1 is correlated with *Y* and *dem*, while entropy is correlated with *corr_sd. Dem_sd* correlates with measures that describe topographical heterogeneity (i.e. *vrm, vrm_sd*), but also variation in temperature. As we do not allow the models to consider all predictors, (we have too few data points for this) multicollinearity is only a problem when parameters from the same "theme" (climate, topography, habitat heterogeneity) are considered.

Step 4. We continue with building the GAM models. For this, we create a null model, which uses only the mean richness value per cell. We will use the null model for baseline comparisons. No model should be worse than a null model. Then, we calculate a model for each single parameter but always including the spatial interaction of the coordinates as this has several advantages such as reduced SAC, cleaner residuals, and better predictive performance. The spatial interactions accounts for large-scale trends in unmeasured parameters.
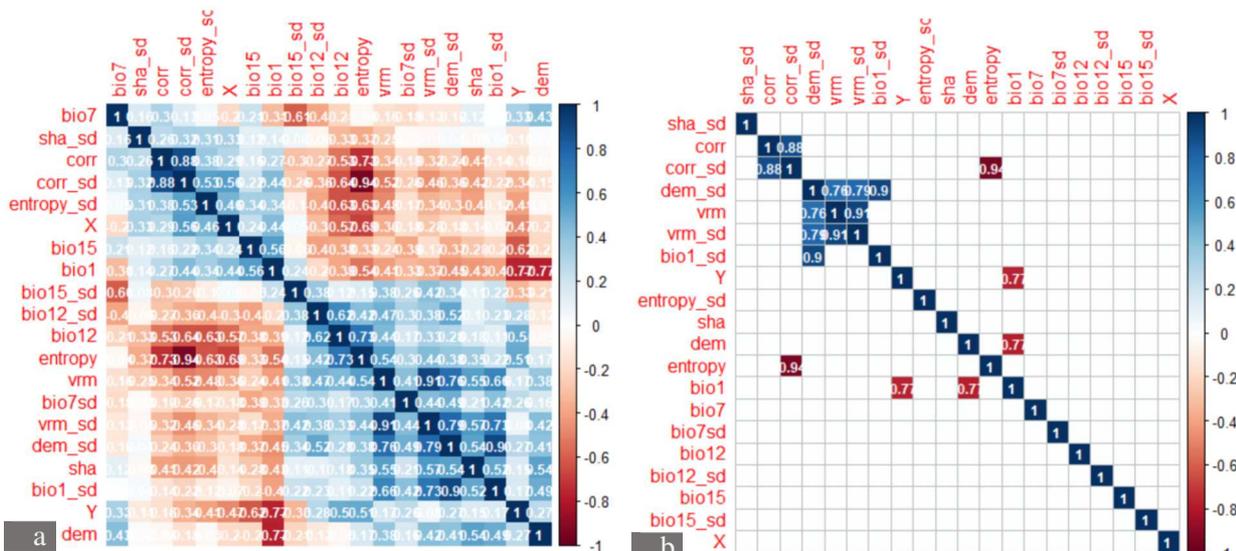

Figure S 1. The multicollinearity analysis using Pearson's correlation coefficient to find the correlated predictors. a) the complete multicollinearity analysis. b) The analysis exclude correlation coefficient less than 0.75.

```
### GAM models ----------
### null model
S.intercept <- gam(Sobs ~ 1, data = envonly, family = "nb", method = "RE
```

```r
ML", select = TRUE)
### single parameter models
S.bio1 <- gam(Sobs ~ s(X, Y, bs = "sos") + s(bio1) , data = envonly, fam
ily = "nb", method = "REML", select = TRUE)
S.bio12 <- gam(Sobs ~ s(X, Y, bs = "sos") + s(bio12) , data = envonly, f
amily = "nb", method = "REML", select = TRUE)
S.bio7 <- gam(Sobs ~ s(X, Y, bs = "sos") + s(bio7) , data = envonly, fam
ily = "nb", method = "REML", select = TRUE)
S.bio15 <- gam(Sobs ~ s(X, Y, bs = "sos") + s(bio15) , data = envonly, f
amily = "nb", method = "REML", select = TRUE)
S.dem <- gam(Sobs ~ s(X, Y, bs = "sos") + s(dem) , data = envonly, famil
y = "nb", method = "REML", select = TRUE)
S.entropy <- gam(Sobs ~ s(X, Y, bs = "sos") + s(entropy) , data = envonl
y, family = "nb", method = "REML", select = TRUE)
S.corr <- gam(Sobs ~ s(X, Y, bs = "sos") + s(corr) , data = envonly, fam
ily = "nb", method = "REML", select = TRUE)
S.sha <- gam(Sobs ~ s(X, Y, bs = "sos") + s(sha) , data = envonly, famil
y = "nb", method = "REML", select = TRUE)
S.vrm <- gam(Sobs ~ s(X, Y, bs = "sos") + s(vrm) , data = envonly, famil
y = "nb", method = "REML", select = TRUE)
### thematic models
S.clim <- gam(Sobs ~ s(X, Y, bs = "sos") + s(bio1) +s(bio12) + s(bio7) +
s(bio15) , data = envonly, family = "nb", method = "REML", select = TR
UE)
S.topo <- gam(Sobs ~ s(X, Y, bs = "sos") + s(dem) + s(sha) + s(vrm) , da
ta = envonly, family = "nb", method = "REML", select = TRUE)
S.hetero <- gam(Sobs ~ s(X, Y, bs = "sos") + s(entropy) + s(corr) , data
 = envonly, family = "nb", method = "REML", select = TRUE)
```

Step 5. After model building, we will evaluate the models by calculating the AIC for each model, sorting these according to delta AIC values and add the Akaike Weights for better interpretation. Further, we will calculate D², a synonym for R² in a generalized model context.

```r
# build AIC table
Sobs.models <- list(S.intercept = S.intercept,
S.bio1 = S.bio1,
S.bio12 = S.bio12,
S.bio7 = S.bio7,
S.bio15 = S.bio15,
S.dem = S.dem,
S.entropy = S.entropy,
S.corr = S.corr,
S.vrm = S.vrm,
S.sha = S.sha,
S.clim = S.clim,
S.topo = S.topo,
S.hetero = S.hetero)

### calculate model summary
tmp.glance <-plyr::ldply(Sobs.models,glance)
tmp.d2 <-plyr::ldply(Sobs.models,Dsquared)
```

```
tmp.glance$D2<-round(tmp.d2[,2],3)
tmp.glance

#make AIC tab
Sobs.AIC<-AICtab(Sobs.models)
Sobs.AIC$AW<- round(Weights(Sobs.AIC$dAIC),3)

Sobs.AIC$df <- round(Sobs.AIC$df,3)
Sobs.AIC

### summary table
summary(S.hetero)
```

The best model at this scale was the thematic model of habitat heterogeneity. The following model summary shows the significance of the smoothers as well as further information on the model (Table S 2).

Step 6. We will now predict the model to the hexagonal grid and compare the observed and predicted values.

```
##create new dataframe to predict to
newdf = hex_env[c("X","Y","entropy","corr")]
newdf <- st_drop_geometry(newdf)
newdf <- as.data.frame(newdf)

## predict on the response scale (richness counts)
hex_env$predS<-predict.gam(object=S.hetero, newdata = newdf,type="respon
se")

## plot the observed and predicted pattern
plot(hex_env[c("Sobs","predS")])

## compare the summary values
summary(hex_env$Sobs) # Observed reptile richness

summary(hex_env$predS) # Predicted reptile richness
```


Figure S 2. The distribution map of the occurrence records based on the observed data (a) and predicted data (b) at 4000 km2 scale.

```
## correlation between predicted and observed
cor.test(hex_env$predS, hex_env$Sobs,method = "pearson")
```

```
## plot the relationship
scatter.smooth(hex_env$Sobs,hex_env$predS, lpars=list(col="red", lwd=3,l
ty=2),
xlab="predicted",ylab="observed")
```
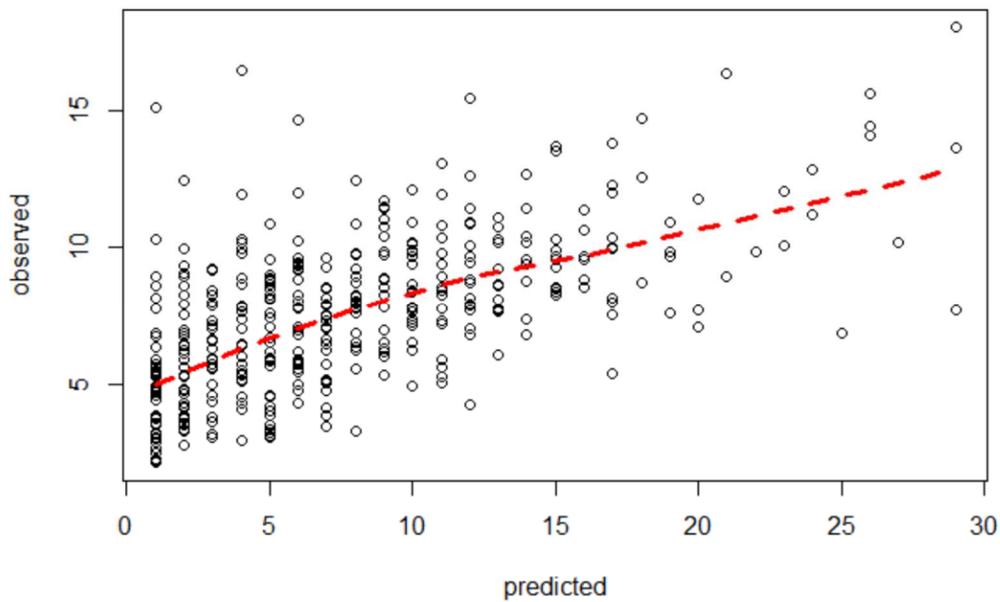

Figure S 3. The graph shows the correlation between observed and our prediction for distribution for the reptile species in Iran.

Step 7. Now we need to assess the validity of the model using diagnostic plots and displays of the smoothers.

```
## using methods from the gratia package
## diagnostic plots
```
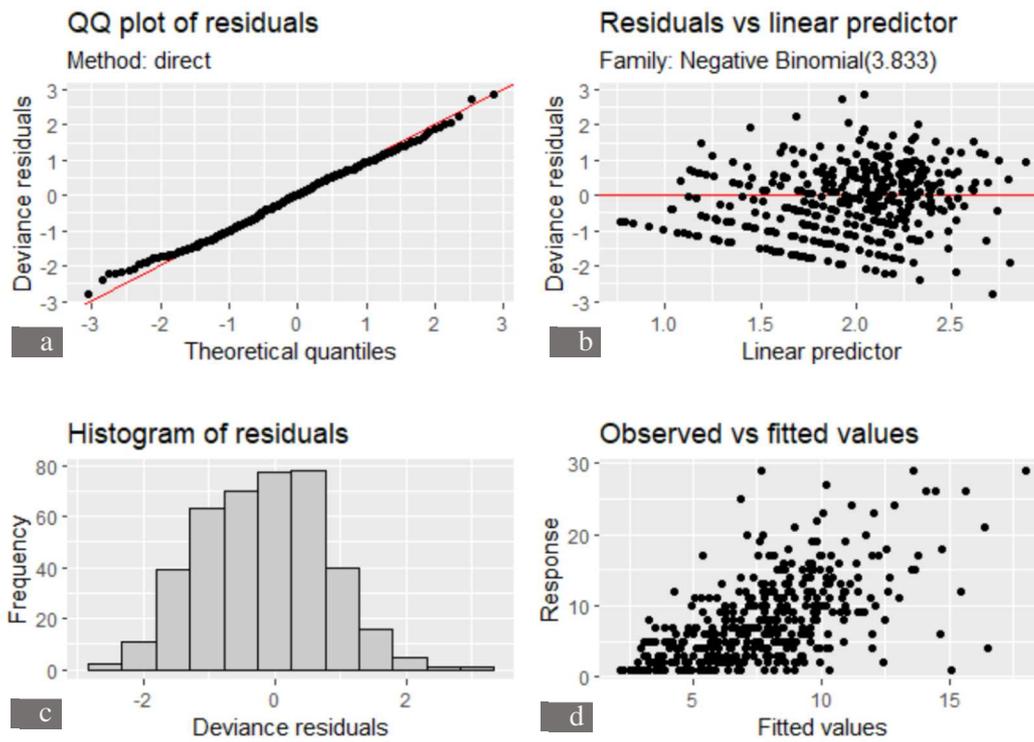
15

```
appraise(S.hetero)
```


Figure S 4. The evaluation for residual model structure of the best model using diagnostic plots. a) QQ-plots. b & d) leverage plots. c) Histogram plot.

```
## plot the smoothers
draw(S.hetero,residuals = F)
```
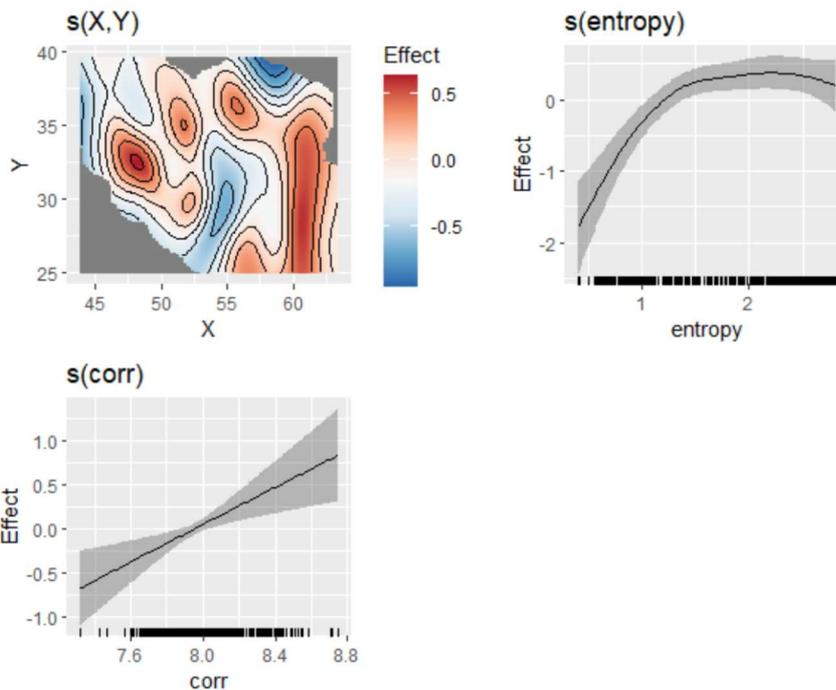

Figure S 5. Univariate and spatial partial regression plots to interpret better the models.

16

Step 8. Here, the diagnostic plots look good. However, as we are doing spatial explicit modelling, we should now check the model residuals for potential effects of spatial autocorrelation.

```
### extract the residuals
E<-(resid(S.hetero,type="scaled.pearson"))
newdf2 <- newdf ## make copy of newdf
mydata <- data.frame(E=E, X=newdf2$X,Y=newdf2$Y)
coordinates(mydata) <- ~ X + Y
proj4string(mydata) = CRS("+init=epsg:4326") ## set WGS84 as CRS

### mydata is now spatial object
## bubble plot
bubble(mydata,"E")
```


Figure S 6. Analysis of the model residuals by plotting the residuals on a map to check for potential effects of spatial autocorrelation (SAC).

```
## isotropic variogram
E.vgm<- variogram(E~ X+Y, mydata)
E.vgm

E.fit = fit.variogram(E.vgm, model = vgm(1, "Sph", 900, 1))
E.fit

plot(E.vgm, E.fit)


## anisotropic variogram
E.vgm<- variogram(E~ X+Y, mydata, alpha=c(0,45,90,135))
E.vgm
```
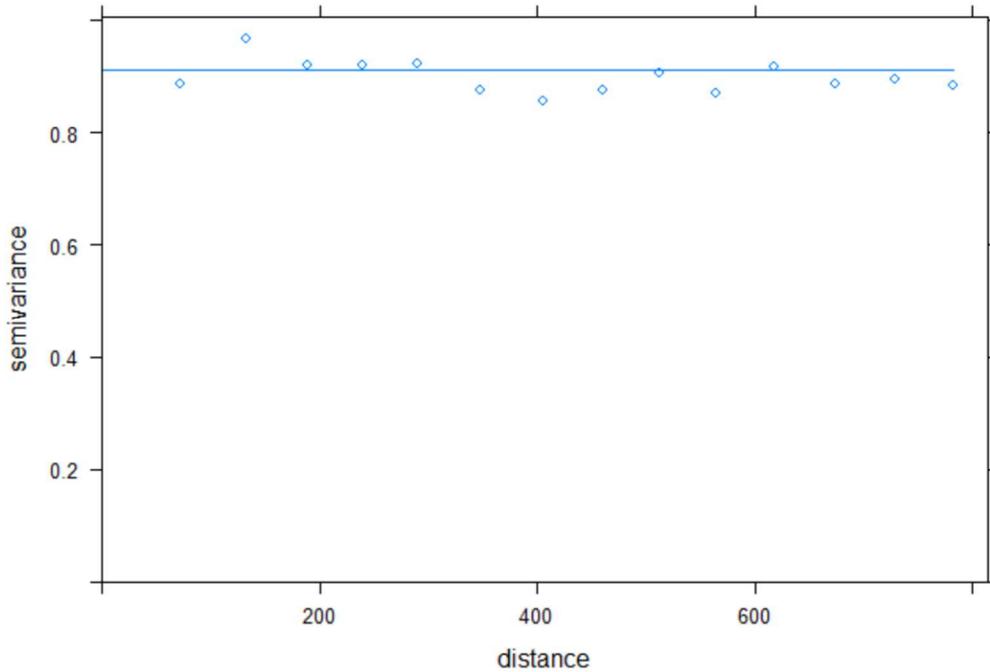
Figure S 7. Analysis of the model residuals by calculating isotropic, as well as anisotropic semi-variograms to check for potential effects of spatial autocorrelation (SAC).

```
E.fit = fit.variogram(E.vgm, model = vgm(1, "Sph", 900, 1, anis = c(45,
0.5)))
E.fit

plot(E.vgm, E.fit)
```
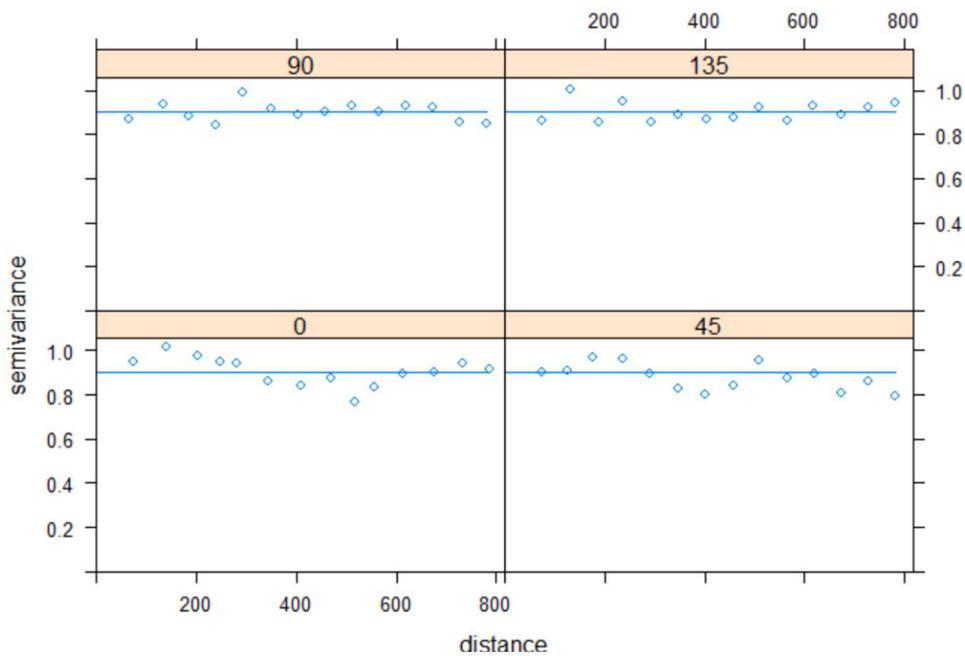

Figure S 8. Analysis of the model residuals by calculating isotropic, as well as anisotropic semi-variograms for the directions (0, 45, 90, and 135) to check for potential effects of spatial autocorrelation (SAC).

```
### Morans'I Correlogram
```

18

```
ncf.cor <- correlog(mydata$X, mydata$Y, mydata$E, increment=100,
resamp=999,latlon=T)

#### number of samples per lag and mean distance of lag in km
ncf.cor$n # number of observations per lag

ncf.cor$mean.of.class # mean km per lag

### plotting the correlogram
plot(ncf.cor, ylim=c(-0.3,0.3))
abline(h=0); abline(h=-0.1, col="red", lty=2); abline(h=0.1, col="red",
lty=2)
```
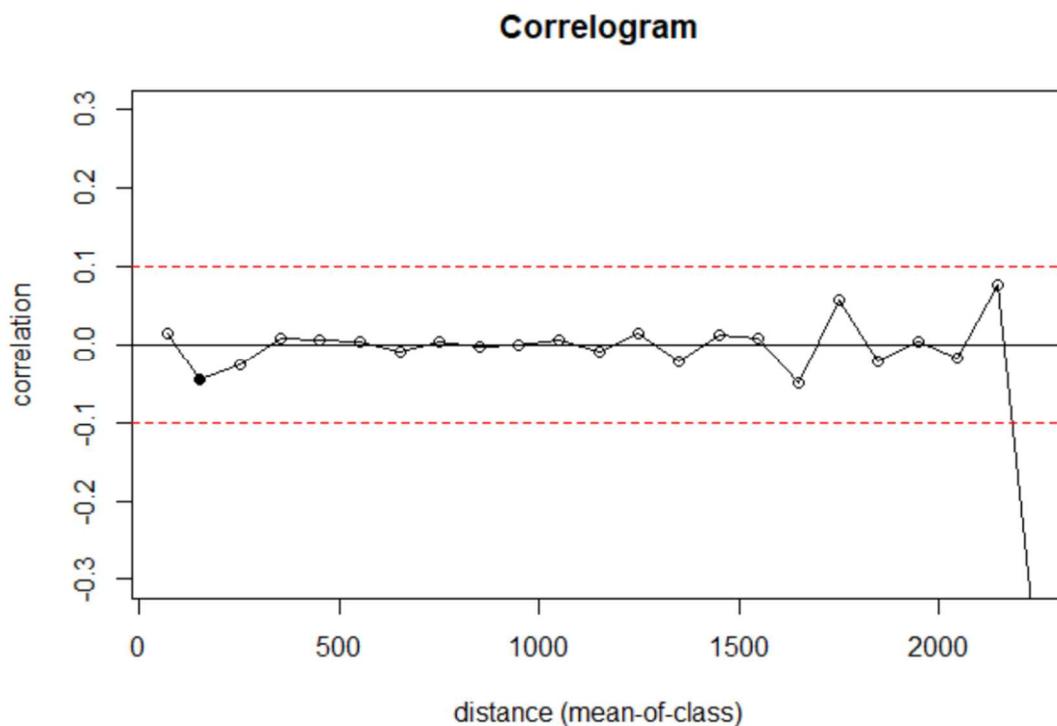
Correlogram

Figure S 9. Calculation a Moran's I spatial correlogram to verify whether SAC had a strong influence at a certain distance (lag). Lags were measured in kilometres and distributed in 50 bins across the spatial extent of the study area.

The model did not show any specific SAC pattern in the residuals. Hence, we can conclude that this is a clean best model we can derive from the given candidate data set. We will save the model in an extra object, so we can reuse the object names.

```
### save model to final object
best4000 <- S.hetero

Step 9. The best model for each scale has been saved for coparison

best20000 <- S.entropy
tab_model(best4000, best8000, best20000, transform = NULL,
show.df=F,
show.se=F,
show.ci=F,
show.dev = T,
dv.labels=c("S_4K", "S_8K","S_20K"))
```